THE UNIVERSITY *of* EDINBURGH

Edinburgh Research Explorer

Design, synthesis and in vivo study of novel pyrrolidine-based 11-HSD1 inhibitors for age-related cognitive dysfunction

OPEN ACCESS

Accepted Manuscript

Design, synthesis and *in vivo* study of novel pyrrolidine-based 11β-HSD1 inhibitors for age-related cognitive dysfunction

Rosana Leiva, Christian Griñan-Ferré, Constantí Seira, Elena Valverde, Andrew McBride, Margaret Binnie, Belén Pérez, F. Javier Luque, Mercè Pallàs, Axel Bidon-Chanal, Scott P. Webster, Santiago Vázquez

GRAPHICAL ABSTRACT

Design, synthesis and *in vivo* study of novel pyrrolidine-based 11β-HSD1 inhibitors for age-related cognitive dysfunction

Rosana Leiva[a], Christian Griñan-Ferré[b], Constantí Seira[c], Elena Valverde[a], Andrew McBride[d], Margaret Binnie[d], Belén Pérez[e], Mercè Pallàs[b], Axel Bidon-Chanal[c], Scott P. Webster[d,*] and Santiago Vázquez[a,*]

[a]*Laboratori de Química Farmacèutica (Unitat Associada al CSIC), Facultat de Farmàcia i Ciències de l'Alimentació, and Institute of Biomedicine (IBUB), Universitat de Barcelona, Av. Joan XXIII 27-31, Barcelona, E-08028, Spain*
[b]*Unitat de Farmacologia, Farmacognòsia i Terapèutica, Facultat de Farmàcia i Ciències de l'Alimentació i Institut de Neurociències, Universitat de Barcelona, Av. Joan XXIII, 27-31, 08028 Barcelona, Spain*
[c]*Department of Nutrition, Food Science and Gastronomy, Faculty of Pharmacy and Institute of Biomedicine (IBUB), Universitat de Barcelona, Av. Prat de la Riba 171, Santa Coloma de Gramenet E-08921, Spain*
[d]*Centre for Cardiovascular Science, University of Edinburgh, Queen's Medical Research Institute, EH16 4TJ, United Kingdom*
[e]*Departament de Farmacologia, Terapèutica i Toxicologia, Universitat Autònoma de Barcelona, 08193 Bellaterra, Barcelona, Spain*

Design, synthesis and *in vivo* study of novel pyrrolidine-based 11β-HSD1 inhibitors for age-related cognitive dysfunction

Rosana Leiva[a], Christian Griñan-Ferré[b], Constantí Seira[c], Elena Valverde[a], Andrew McBride[d], Margaret Binnie[d], Belén Pérez[e], F. Javier Luque[c], Mercè Pallàs[b], Axel Bidon-Chanal[c], Scott P. Webster[d,*], and Santiago Vázquez[a,*]
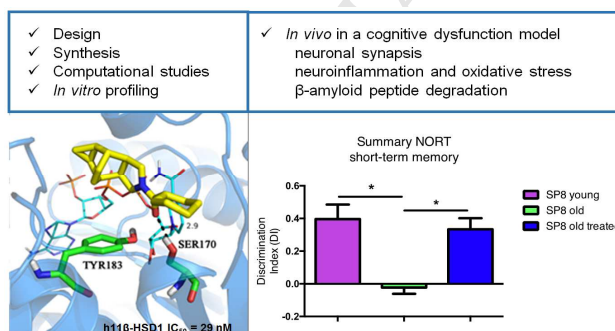
[a]*Laboratori de Química Farmacèutica (Unitat Associada al CSIC), Facultat de Farmàcia i Cienciès de l'Alimentació, and Institute of Biomedicine (IBUB), Universitat de Barcelona, Av. Joan XXIII 27-31, Barcelona, E-08028, Spain*

[b]*Unitat de Farmacologia, Farmacognòsia i Terapèutica, Facultat de Farmàcia i Ciències de l'Alimentació i Institut de Neurociències, Universitat de Barcelona, Av. Joan XXIII, 27-31, 08028 Barcelona, Spain*

[c]*Department of Nutrition, Food Science and Gastronomy, Faculty of Pharmacy and Institute of Biomedicine (IBUB), Universitat de Barcelona, Av. Prat de la Riba 171, Santa Coloma de Gramenet E-08921, Spain*

[d]*Centre for Cardiovascular Science, University of Edinburgh, Queen's Medical Research Institute, EH16 4TJ, United Kingdom*

[e]*Departament de Farmacologia, Terapèutica i Toxicologia, Universitat Autònoma de Barcelona, 08193 Bellaterra, Barcelona, Spain*

[*]Corresponding authors. Tel.: Phone: +44 1312426738. E-mail: scott.webster@ed.ac.uk; Phone : +34-934-024-533; e-mail: svazquez@ub.edu

Abstract:

Recent findings suggest that treatment with 11β-HSD1 inhibitors provides a novel approach to deal with age-related cognitive dysfunctions, including Alzheimer's disease. In this work we report potent 11β-HSD1 inhibitors featuring unexplored pyrrolidine-based polycyclic substituents. A selected candidate administered to 12-month-old SAMP8 mice for four weeks prevented memory deficits and displayed a neuroprotective action. This is the first time that 11β-HSD1 inhibitors have been studied in this broadly-used mouse model of accelerated senescence and late-onset Alzheimer's disease.

Keywords:

Glucocorticoids, 11β-HSD1 inhibitors, drug design, adamantane, polycyclic substituents, aged-related cognitive dysfunction, Alzheimer's disease, SAMP8 mouse.

Highlights:

a)   Several pyrrolidine-based polycyclic amides are prepared as 11β-HSD1 inhibitors.

b)   Amides are synthesized by coupling of pyrrolidines with carboxylic acids.

c)   The more potent compounds present low nanomolar IC_{50}.

d)   A candidate is administered to old SAMP8 mice for four weeks.

e)   The treatment prevents memory deficits and displays a neuroprotective action.

1. Introduction

Elevated glucocorticoids (GCs) exposure is widely accepted as a key factor in age-related cognitive decline in rodents and humans [1-3]. High levels of GCs have been found in elderly individuals who exhibit learning and memory impairments. GC levels correlate with greater hippocampal atrophy, a region of the brain that is crucial for memory formation [3]. In contrast, low GC levels achieved through neonatal programming or adrenalectomy with exogenous steroid replacement in rats results in the prevention of memory impairments with aging [4].

Growing evidence also suggests that excessive glucocorticoid activity may contribute to Alzheimer's disease (AD), since elevated levels of circulating cortisol in AD patients are associated with more rapid disease progression [5-6]. In a rodent model of AD, systemic administration of GCs led to increases in β-amyloid and tau pathology, the two major histopathologic hallmarks of AD, suggesting a relationship between elevated GC levels and AD pathology [7]. Overall, these data suggest that reducing GC levels in the brain may relieve cognitive dysfunction in both aging and AD.

As in other tissues, the presence of GCs in the brain is not only dependent on adrenal secretion and diffusion from the circulation but also on intracellular metabolism [8]. 11β-hydroxysteroid dehydrogenase type 1 (11β-HSD1) catalyzes the regeneration of active GCs (cortisol in humans, corticosterone in rodents) from their inactive forms (cortisone and 11-dehydrocorticosterone, respectively), providing a local amplification of GC action [9-10]. 11β-HSD1 is highly expressed in fundamental brain areas for cognition, such as the hippocampus, cortex and amygdala [11-13]. By contrast, the isoenzyme 11β-hydroxysteroid dehydrogenase type 2 (11β-HSD2), which catalyzes the opposite reaction, plays an important role during development, as expression of 11β-HSD2 is relevant in fetal brain and placenta, but it has very limited expression in the adult brain [14-16].

Recent studies have demonstrated that aged mice with cognitive deficits show increased 11β-HSD1 expression in the hippocampus and forebrain, and that overexpression of 11β-HSD1 leads to a similar premature memory decline [17]. Conversely, 11β-HSD1 knock-out mice and even heterozygous null mice performed better in different behavioral tests, which suggests resistance to cognitive decline due to a neuroprotective effect of 11β-HSD1 inhibition [18]. Accordingly, this protection correlates with loss of the age-associated rise in intrahippocampal corticosterone, insinuating a role for 11β-

HSD1 in maintaining plasma corticosterone concentration [17]. Furthermore, acute and short-term treatments with 11β-HSD1 inhibitors have shown memory consolidation and improvements in cognitive function in aged mice and AD models [19-23]. Altogether, these findings suggest that 11β-HSD1 inhibitors provide a novel approach through a non-cholinergic mechanism to deal with these cognitive disorders.

In the present work, we report the results derived from a synthetic strategy, supported by molecular modeling studies, designed towards a novel family of potent 11β-HSD1 inhibitors, featuring unexplored pyrrolidine-based polycyclic substituents. The more potent compounds were characterized in terms of cellular potency, isoenzyme selectivity, human metabolic stability and predicted brain penetration to select a candidate for an *in vivo* study. For the first time in the context of 11β-HSD1 inhibitors, the Senescence Accelerated Mouse-Prone 8 (SAMP8) mice were used, as a naturally occurring mouse strain that displays a phenotype of accelerated aging as observed in AD and widely used as a robust rodent model of cognitive dysfunction [24-25].

2. Design, synthesis and *in vitro* evaluation of new inhibitors

Given that the 11β-HSD1 active site includes a hydrophobic pocket that can accommodate bulky lipophilic substituents, the introduction of a lipophilic group, such as adamantyl, has proven a successful strategy for the space filling of the cavity. Thus, several adamantyl-containing 11β-HSD1 inhibitors exhibit high affinity and potency and some of them (e.g. AZD8329 and ABT-384) have reached clinical trials (Figure 1) [26-34]. Although the evaluation of alternative polycyclic hydrocarbons may offer further opportunities for optimizing the space filling of the hydrophobic cavity, the use of other polycyclic substituents featuring different size or shape has only been briefly scrutinized (e.g. AMG-221 and MK-0736) [35-36].
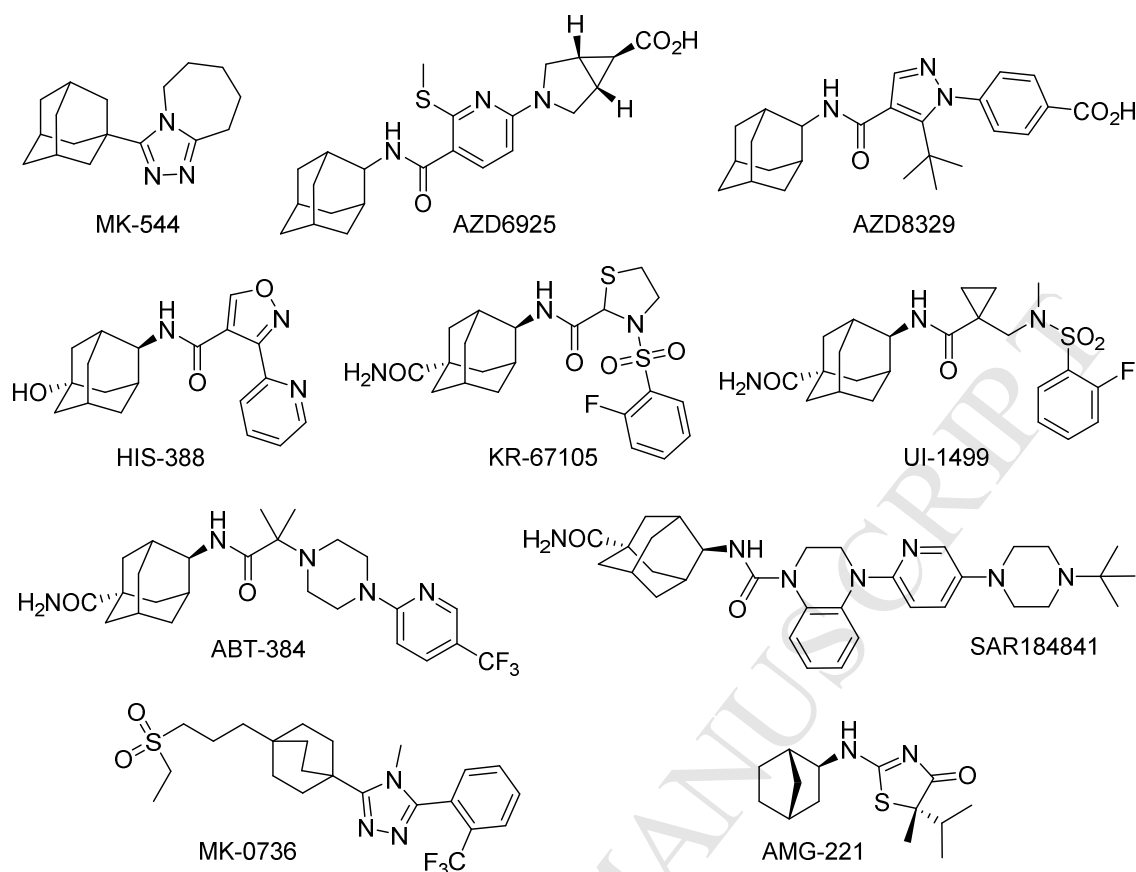
Figure 1. Selected 11β-HSD1 inhibitors.

In the last few years, our research group has investigated new polycyclic substituents as surrogates of the adamantyl group, leading to inhibitors with promising results on multiple targets [37-45]. However, this strategy has not been successful yet in the case of human 11β-HSD1 inhibitors [46]. Very recently, we have found that the *N*-(2-adamantyl)amide derivatives **1** and **2** (Figure 2), which are achiral analogues of PF-877423 (IC$_{50}$ = 4 nM) [47], are potent inhibitors of 11β-HSD1 (IC$_{50}$ = 86 and 74 nM, respectively) [48]. Interestingly, the corresponding urea analog, **3**, was significantly less potent (IC$_{50}$ = 873 nM) [48]. Taking into account the simplicity of these three right-hand side (RHS) units, here we initially selected these fragments for finding alternative polycyclic substituents able to successfully replace the adamantyl group in 11β-HSD1 inhibitors.
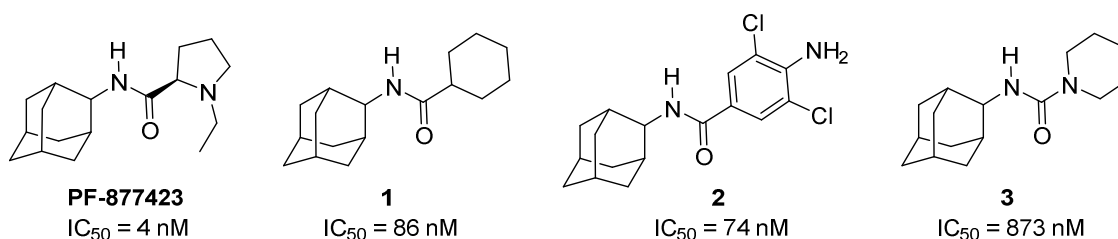
Figure 2. PF-877423 and related inhibitors.

The design of new inhibitors was initially based on a structure-activity relationship (SAR) investigation we previously adopted [46]. The structure of the putative inhibitor was partitioned into two parts: the polycyclic substituent, a surrogate of adamantyl, and the carbocyclic or heterocyclic ring, linked by an amido or urea unit, respectively. Since inspection of the available X-ray structures and preliminary docking studies (see below) indicated that the enzyme active site is large enough to accommodate a polycycle bigger than adamantane, we started our endeavour with previously synthesized amines **4**, **5** and **10**, three compounds that were successfully used to replace 1-adamantylamine in other targets (Scheme 1) [38]. These amines were then combined with a common RHS moiety to shed light on the effect of key structural features on the inhibitory action: i) primary *vs* secondary amine (e.g. **4** *vs* **10**), ii) distance between the polycyclic ring and the nitrogen atom (e.g. **4** *vs* **5**), iii) restraint of the conformational freedom (e.g. **5** *vs* **10**), and iv) by incorporating two double bonds in the polycycle, which might form additional interactions in the binding site (e.g. derivatives of **10** *vs* its reduced analogues). Amides **6** and **7** were prepared in high yields by reaction of cyclohexane acyl chloride with amines **4** and **5**, respectively. From amine **10**, using either cyclohexanecarboxylic acid or 4-amino-3,5-dichlorobenzoic acid in combination with 1-hydroxybenzotriazole (HOBt) and *N*-(3-dimethylaminopropyl)-*N'*-ethylcarbodiimide (EDC) amides **11** and **15** were synthesized in moderate yields. Ureas **8**, **9** and **13** were prepared from the required amine and *N*-chloroformylpiperidine in moderate to excellent yields. Finally, catalytic hydrogenation of **11**, **13** and **15** furnished **12**, **14** and **16**, respectively (Scheme 1).
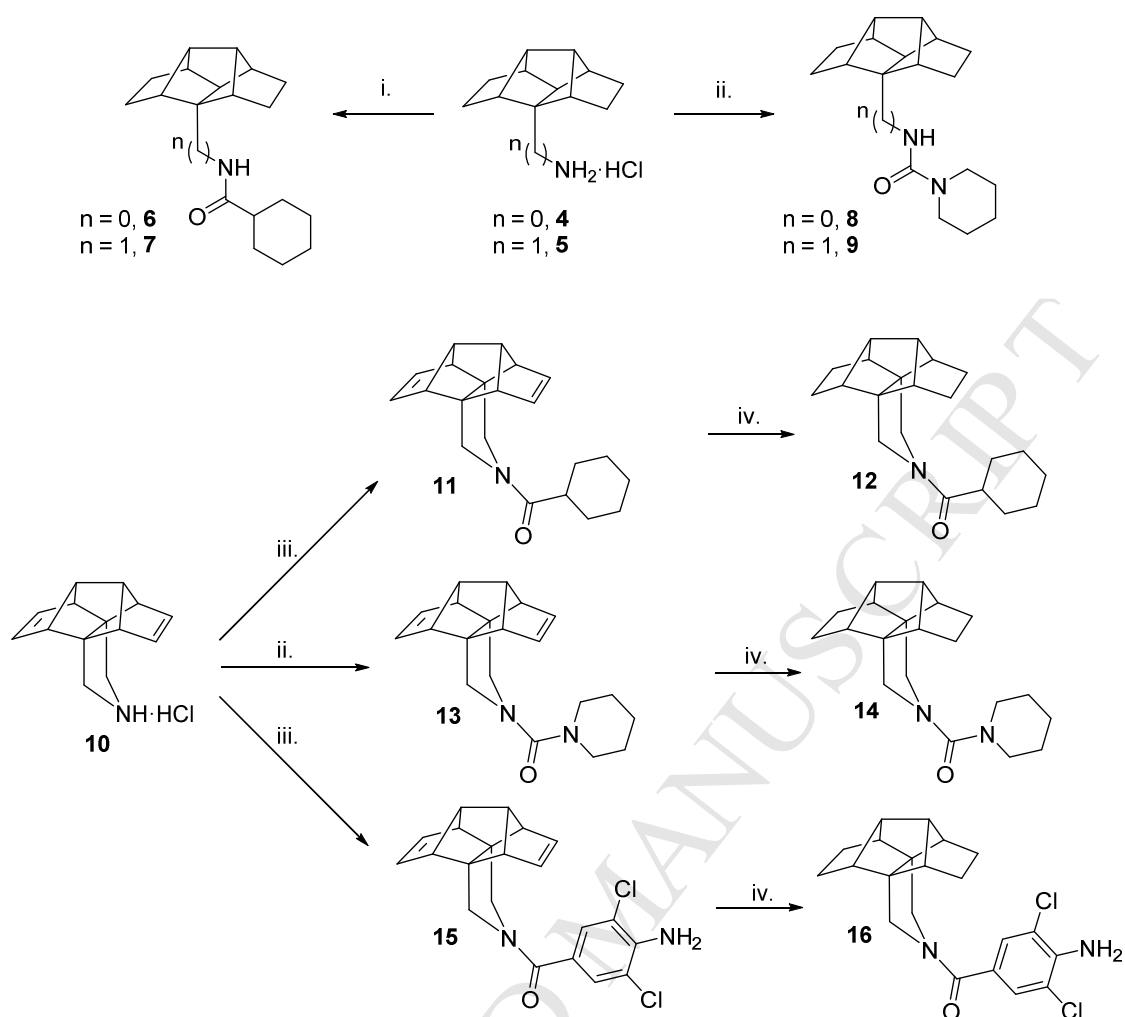
Scheme 1. Amines 4, 5 and 10, and amides and ureas derived thereof. [a]

[a]Reagents and conditions: (i) cyclohexanecarbonyl chloride, anh. acetone, reflux, 3 h, 95% yield for **6**; 78% yield for **7**; (ii) 1-piperidinecarbonyl chloride, Et$_3$N, DCM, rt, overnight, 54% yield for **8**; quant yield for **9**; 71% for **13**; (iii) cyclohexanecarboxylic acid for **11** or 4-amino-3,5-dichlorobenzoic acid for **15**, HOBt, EDC, Et$_3$N, EtOAc, rt, overnight, 42% yield for **11**; 47% yield for **15**; (iv) H$_2$, Pd/C, abs. EtOH, rt, 5 h for **12** and **16**, 3 h for **14**, 78% yield for **12**; 72% yield for **14**; 89% yield for **16**.

A preliminary *in vitro* microsomal assay at 10 µM compound concentration was performed to assess if the synthesized compounds were able to inhibit human 11β-HSD1, and the IC$_{50}$ values were determined for those compounds presenting an inhibition higher than 50% (Table 1).

Compound	hHSD1 % inh at 10 µM	hHSD1 IC_{50} (µM)
6	41	ND
7	28	ND
8	50	ND
9	50	ND
11	95	1.08
12	100	0.29
14	100	0.32
15	98	2.77
16	98	0.41

Table 1. 11β-HSD1 inhibition by compounds 6-9, 11, 12 and 14-16. [a,b]

[a]11β-HSD1 inhibition was determined in mixed sex, human liver microsomes (Celsis In-vitro Technologies) by measuring the conversion of ^{3}H-cortisone to ^{3}H-cortisol in a cortisol-scintillation proximity assay. [b]Percentage inhibition was determined relative to a control system in the absence of inhibitor (see Experimental section for further details). ND, not determined.

The analysis of the inhibitory potencies disclosed some SAR. First, while amides **6** and **7** displayed poor inhibitory activity, derivatives **11** and **12**, featuring a pyrrolidine ring, showed low micromolar and submicromolar potency, respectively, reflecting a better fit within the hydrophobic pocket of the binding site. Second, replacement of the cyclohexyl ring of **12** by either a 1-piperidinyl substituent, as in **14**, or a 4-amino-3,5-dichlorophenyl group, as in **16**, retained the activity, further demonstrating that the adamantyl substituent may be replaced by other polycyclic groups. Third, no significant difference was found between the inhibitory activity of **12** and **14**, and hence the replacement of the amide bridge by a urea within this particular polycycle does not seem to affect the potency. Finally, saturated hexacyclic pyrrolidines were more potent than their diene analogues (compare **12** *vs* **11** and **16** *vs* **15**). Overall, aliphatic amides **11** and **12** were slightly more potent than aromatic amides **15** and **16** (compare **11** *vs* **15** and **12** *vs* **16**).
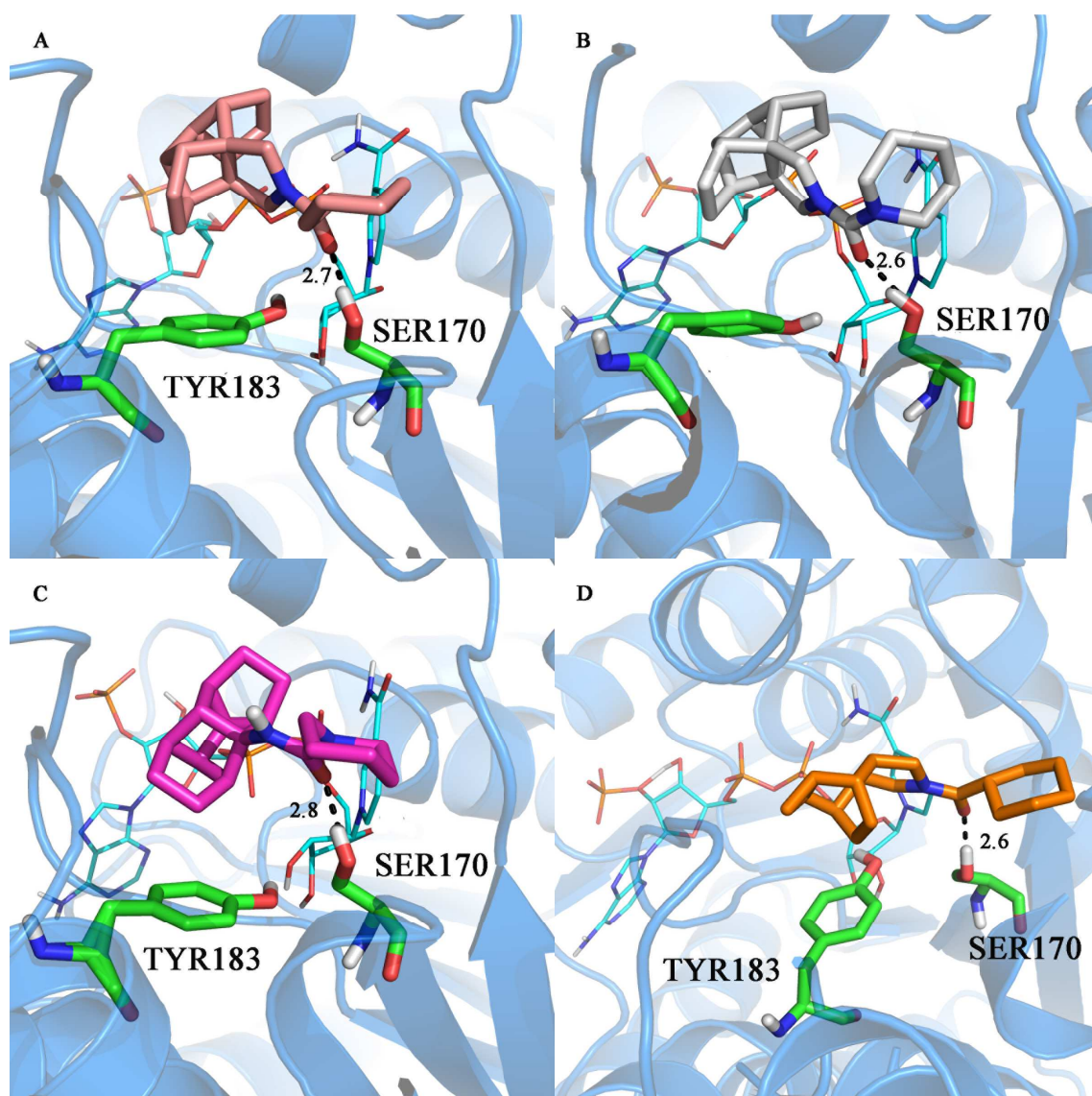
Figure 3. Representative snapshot of the binding mode of compounds **12** (A), **14** (B), **8** (C), and **23** (D) to the human 11β-HSD1 enzyme as determined from the analysis of the MD simulations. The protein backbone is shown as blue carton, the NADP cofactor, residues Tyr183 and Ser170, and the ligands are shown as atom-coloured sticks. The hydrogen bond between the ligand and the hydroxyl group of Ser170 is shown as a dashed line.

Docking studies were combined with molecular dynamics (MD) simulations to shed light into the inhibitory potencies of selected compounds. The structural integrity of the simulated systems was supported by the stability of the positional root-mean square deviation of the residues that define the binding site and the ligand, especially for the most potent compounds (see Figures S1-S3 in Supporting Information). A similar

binding mode was found for compounds **8**, **12** and **14** (see Figure 3). In all cases the carbonyl group of the ligand formed a stable hydrogen bond with Ser170 (distances ranging from 2.6 to 3.0 Å). However, the hydrogen bond of the ligand's carbonyl group with the hydroxyl group of Tyr183, which was retained during the setup of the simulated systems, exhibited larger fluctuations and was eventually disrupted during the trajectories. Docking calculations showed compounds **12** and **14** to have slightly better scores (-9.3 and -9.7 kcal/mol, respectively) than for **6** (-8.4 kcal/mol) and **8** (-9.0 kcal/mol). The higher inhibitory potency of **12** and **14** may also be explained by the fused pyrrolidine ring, which should reduce the contribution of the conformational penalty to the binding affinity of these compounds compared to the more flexible compounds **6** and **8**. Although the results appear to support the ability of the size-expanded hydrophobic cage present in **12** and **14** to occupy the binding pocket, the lower inhibitory potency compared to **1** (IC$_{50}$ = 86 nM; Figure 2) suggests that the size of the polycyclic substituent in **12** and **14** may be close to the upper limit allowed for ligand binding without triggering significant structural distortions in the pocket

Of note, the *N*-acylpyrrolidine motif contained in **11**, **12**, **15** and **16** has scarcely been explored in the context of the design of 11β-HSD1 inhibitors [49]. However, the pyrrolidine **10** is not an ideal starting compound for a medicinal chemistry program, as its synthesis is tedious and very low-yielding [38]. For this reason, we explored the synthesis of alternative, easily synthesized, pyrrolidine derivatives. To this end, we followed a polycyclic substituent optimization process in which the cyclohexyl was selected as the RHS of the molecule, due to its simplicity (i.e. achiral, easy access) and good performance with both adamantyl (**1**, IC$_{50}$ = 0.09 μM) and hexacyclic substituents (**12**, IC$_{50}$ = 0.29 μM). An array of 13 pyrrolidine-based polycyclic amides was prepared from cyclohexanecarboxylic acid, HOBt, EDC, and a series of previously synthesized amines (Figure 4). Our aim was to obtain different pyrrolidine-based polycyclic compounds, some of them simplified analogs of the hexacyclic unit contained in **10** but with higher conformational freedom, in order to find the optimal size and shape to deliver more potent 11β-HSD1 inhibitors.
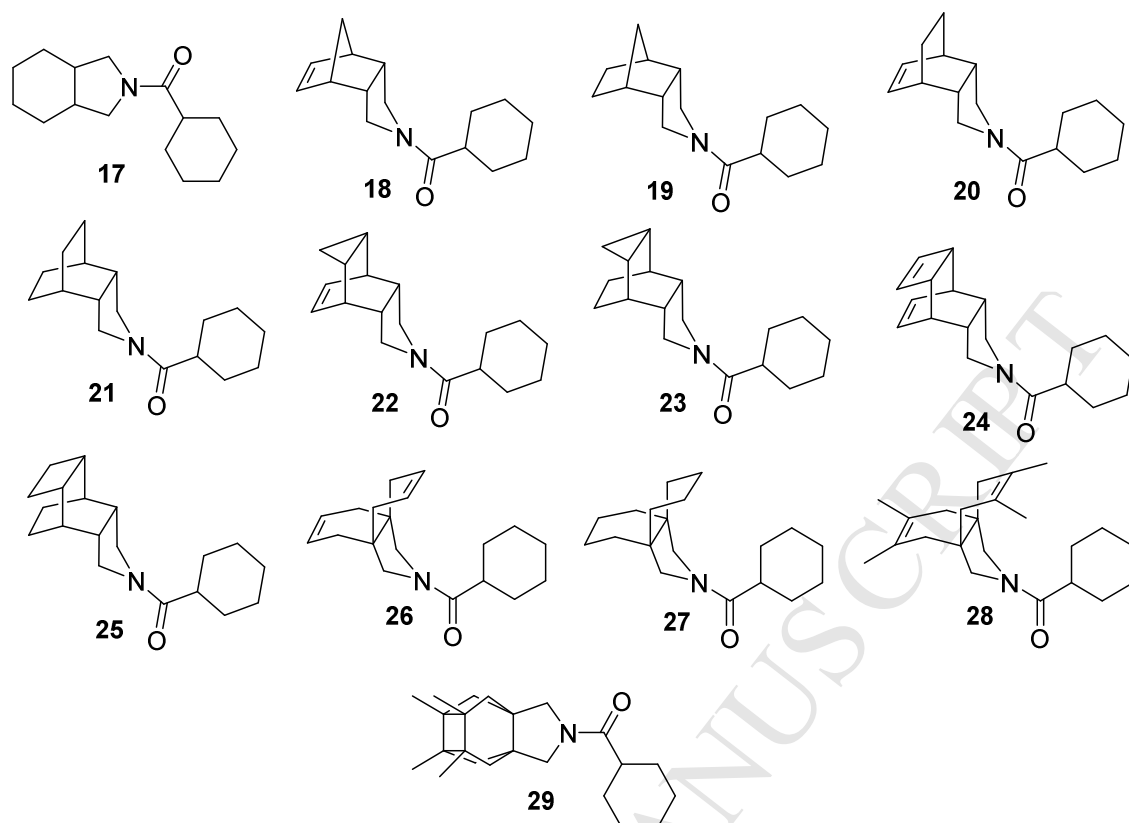
Figure 4. Novel pyrrolidine-based polycyclic amides 17-29.

Following the aforementioned preliminary *in vitro* microsomal assay, the IC$_{50}$ values were determined for compounds with an inhibitory activity higher than 50% at 10 μM (Table 2). In general, compounds containing smaller polycyclic rings (i.e. **17**-**23**) were one order of magnitude more potent than our initially best inhibitors **12**, **14** and **16**, and some of them were also more potent than the adamantyl derivative **1** (IC$_{50}$ = 0.09 μM). The most potent inhibitors were **18**, **20**, **21**, **22** and **23** (IC$_{50}$ values ranging from 0.02 to 0.03 μM). MD simulations of the enzyme complex with compound **23** confirmed the stability of the binding mode (see Figure 3D and S4), which resembled the arrangement of compound **12**, and the formation of the hydrogen-bond interaction with Ser170 (average distance of 2.8 ± 0.3 Å). However, there was not a clear trend in terms of activity between the alkene/alkane pairs containing the same polycyclic ring system (compare **20** *vs* **21**, and **22** *vs* **23**). Thus, in the pair **18**/**19** the alkene derivative presented a slightly higher potency, but the bigger alkene derivatives **24** and **26** were significantly more potent than their alkane analogues **25** and **27** (IC$_{50}$ = 1.49 μM *vs* 27% inhibition at 10 μM, and 0.04 μM *vs* 1.22 μM, respectively). Finally, the introduction of four methyl groups, either in an extended (**28**) or compact (**29**) arrangement, was highly

deleterious to the inhibitory activity (compare **26** *vs* **28** and **29**). Overall, these findings reinforce the assumption that the hexacyclic substituent reaches the upper-limit size to fill the hydrophobic pocket of the binding site.

Compound	hHSD1 % inh at 10 µM	hHSD1 IC$_{50}$ (µM)
17	85	0.05
18	89	0.02
19	92	0.09
20	96	0.03
21	95	0.02
22	100	0.02
23	100	0.03
24	83	1.49
25	27	ND
26	82	0.04
27	67	1.22
28	30	ND
29	42	ND

Table 2. 11β-HSD1 inhibition by compounds 17-29.[a,b]

[a]11β-HSD1 inhibition was determined in mixed sex, Human Liver Microsomes (Celsis In-vitro Technologies) by measuring the conversion of ^{3}H-cortisone to ^{3}H-cortisol in a cortisol-Scintillation Proximity Assay. [b]Percentage inhibition was determined relative to a no inhibitor control (see Experimental section for further details). ND, not determined.

3. Biological profiling of the more potent 11β-HSD1 inhibitors

The more potent inhibitors obtained by this polycyclic substituent optimization process have clogP values between 2.68 and 3.99, more desirable than that of the adamantyl-containing analogue **1** (clogP = 4.65). These new compounds were characterized in terms of cellular potency, selectivity over 11β-HSD2, human metabolic stability, cytochromes P450 (CYP) inhibition and predicted brain permeability, in order to select

the best candidate to perform an *in vivo* study in a rodent model of cognitive dysfunction.

The cellular potency was assessed in Human Embryonic Kidney 293 (HEK293) cells stably transfected with the 11β-HSD1 gene. With the only exception of alkenes **18**, **20** and **26**, which showed a moderate inhibitory activity (55%, 64% and 64%, respectively), all compounds completely inhibited the enzyme at 10 µM (Table 3).

Selectivity over 11β-HSD2 is required for 11β-HSD1 inhibitors progressing into clinical trials since 11β-HSD2 inhibition in the kidney can lead to sodium retention and increased blood pressure *via* cortisol stimulation of mineralocorticoid receptors. However, for the purposes of our *in vivo* studiy of cognitive dysfunction in rodents, high selectivity *vs* 11β-HSD2 was not required. Notwithstanding, 11β-HSD2 inhibition was assessed in a cellular assay with HEK293 cells stably transfected with the 11β-HSD2 gene at 10, 1 and 0.1 µM in order to establish the selectivity of our compounds. Ideally, the 11β-HSD2 inhibition at 10 µM should be lower than 50% to consider a compound sufficiently selective toward 11β-HSD1. None of our compounds achieved this threshold but some slightly improved the poor selectivity of the adamantyl-containing analogue **1**, such as amide **22** (88% *vs* 69% inhibition at 10 µM, respectively, data not shown). Although **22** had an IC_{50} between 1 and 10 µM, so we cannot rigorously consider this compound to be selective against 11β-HSD1, its selectivity index was at least 50-fold compared to compounds **20** and **21,** which displayed selectivities less than 5-fold. Poor selectivity was observed for compounds **18**, **19** and **23**.

Microsomal stability was performed in human liver microsomes (HLM), which are widely used to determine the likely degree of primary metabolic clearance in the liver. Compounds **18**, **19** and **20** presented moderate microsomal stabilities between 36 and 60% of remaining parent compound after 30 min incubation, while amides **21** and **22** showed stabilities lower than 28%. Compound **23** displayed a high microsomal stability with 94% of remaining parent compound after the 30 min incubation period.

The active compounds in the 11β-HSD1 cellular assay (**19** and **21**-**23**) were further tested for predicted brain permeation using the widely used *in vitro* PAMPA-BBB model [50]. Unfortunately, the *in vitro* permeabilities (P_e) for compounds **21** and **22** could not be determined due to their lack of UV absorption. Whereas **19** showed an uncertain BBB permeation [CNS ± with 5.179 > P_e (10^{-6} cm s^{-1}) > 2.106], compound **23**

had P_e clearly above the threshold established for a high blood-brain barrier (BBB) permeation ($P_e > 30 \times 10^{-6}$ cm s^{-1}).

Compound	hHSD1 IC$_{50}$ (µM)	HEK hHSD1 % inh at 10 µM[c]	HEK hHSD2 inhibition at 10 µM or IC$_{50}$ (µM)[c]	HLM % parent[d]	PAMPA-BBB P_e (10^{-6} cm s^{-1})[e,f]
1	0.09	100	88%	79	-
18	0.02	55	< 0.1 µM	60	-
19	0.099	100	< 0.1 µM	37	5.20 ± 0.1 (CNS±)
20	0.03	64	0.1-1 µM	44	-
21	0.02	100	0.1-1 µM	17	ND[g]
22	0.02	100	1-10 µM	27	ND
23	0.03	100	< 0.1 µM	94	>30 (CNS+)
26	0.04	64	100%	-	-

Table 3. Biological profiling of the most potent compounds.[a,b]

[a]See Experimental section for further details. [b]Percentage inhibition was determined relative to a no inhibitor control. [c]HEK293 cells stably transfected with the full-length gene coding for human either 11β-HSD1 or 11β-HSD2 were used. [d]The microsomal stability of each compound was determined using human liver microsomes. [e]Permeability values from PAMPA-BBB assay. Values are expressed as the mean ± SD of three independent experiments. CNS+, predicted positive brain penetration. [f]Calibration line between 0 and 30 x 10^{-6} cm s^{-1}. [g]ND, not detected.

4. *In vivo* study

Recent studies in rodents and humans with brain-penetrant 11β-HSD1 inhibitors have shown that they provide beneficial effects on the cognitive impairment associated with aging [13, 18-23]. SAMP8 has been studied as a non-transgenic murine mouse model of accelerated senescence and late-onset AD [51-52]. These mice exhibit cognitive and emotional disturbances, probably due to early development of brain pathological hallmarks, such as oxidative stress (OS), inflammation, and activation of neuronal death pathways, which mainly affect cerebral cortex and hippocampus [24,53]. To date, this

rodent model has not been used to test 11β-HSD1 inhibitors, being this work the first investigation of the effects of 11β-HSD1 pharmacological inhibition in SAMP8.

The *in vivo* study was performed with amide **23**, as this compound had low nanomolar potency against the murine 11β-HSD1 enzyme (mHSD1, IC_{50} = 0.08 µM), high cellular potency, high microsomal stability (both in human and mouse liver microsomes, 94 and 93%, respectively) and positive predicted brain penetration. A pharmacokinetic study of compound **23** was performed in order to assess its oral administration. Although its clearance seems to be rapid, the concentration levels at 30 min post-administration are five fold the IC_{50} (Table S1, Figure S5 and Table S2). In addition, we could also measure compound concentration in brain tissue at 3 hours post-administration (1.45 ng/mL), hint of *in vivo* BBB permeability. Then, compound **23** was administered to 12-month-old SAMP8 mice in drinking water during four weeks at a concentration of 105 mg/L (average body weight for 48-week-old mice is 25 g; fluid consumption is 5 mL, therefore the dose was 0.105 mg/mL x 5 mL/0.025 kg = 21 mg/kg). Compound **23** was dissolved in polyethylene glycol 400 (PEG400) and then diluted with water to a PEG400 final concentration of 2% (v/v) in drinking fluid. 2% PEG400 in water was given to the remaining mice in drinking fluid as a vehicle control.

Neuroprotective effects were investigated through a behavioural test, the novel object recognition test (NORT), as a common measure of cognition (short-term and long-term memory) [54], and biochemical analysis, which were made through Western blotting and quantitative real-time polymerase chain reaction (qPCR). Brain tissue was analysed upon termination of the study to determine compound levels and *ex vivo* inhibition of 11β-HSD1. Consistent with previous reports, we found that aged SAMP8 mice presented memory impairments in the NORT when compared to young animals [53]. Satisfactorily, treatment with **23** certainly prevented short-term and long-term memory deficits in SAMP8 mice (Figure 5A).

Postsynaptic density 95 (PSD95) protein levels were evaluated as a measure of neuronal synapses, whereas gene expression for interleukin-6 (IL-6), which acts as a pro-inflammatory cytokine, and for inducible nitric oxide synthase (iNOS), an oxidative stress sensor that catalyzes the production of nitric oxide (NO), were also studied. Treatment with **23** prevented the reduction of PSD95 protein levels, while the oxidative stress and pro-inflammatory gene expression markers, such as iNOS and IL-6, were significantly decreased compared to untreated mice (Figure 5A-B). These observations

indicate a neuroprotective action of **23**, whereby reduced cognitive impairment in **23**-treated mice is mediated by a reduction of neuroinflammation and oxidative stress as confirmed by in the measurements of pro-inflammatory biomarkers (IL-6 and iNOS).

AD is characterized by the production and deposition of β-amyloid and it has been postulated that its reduction produces beneficial effects [55]. For these reasons, the effect of **23** in modifying amyloid processing pathways was also examined. No changes in amyloid beta A4 precursor (*Pre*APP), β-secretase 1 (*Bace1*), disintegrin and metalloproteinase 10 (*Adam 10*) gene expression levels were found (data not shown). Nevertheless, after treatment with **23**, we found a decrease of APP β-secretase C-terminal fragment (βCTF) protein levels without modification of those of *Pre*APP, together with an increase of the protein levels of insulin-degrading enzyme (IDE) (Figure 1C), a zinc metalloprotease that degrades β-amyloid species. Several *in vitro* and *in vivo* studies have shown correlations between IDE, β-amyloid levels and AD [56].

In an attempt to elucidate the mechanisms underlying the beneficial effects of **23** and the relationship with cognitive amelioration in old SAMP8, we focused our study on amyloid processing and βCTF because of its implication in neurodegeneration and cognitive decline process in this strain [57]. Amide **23** did not alter the proamiloidogenic pathway in SAMP8, as demonstrated by the lack of effect on *Pre-APP*, *Adam10* or *Bace1* gene expression (see Figure S6 in the Supplementary material file). However, the capacity of the brain to remove proamiloidogenic species by activation of specific proteases, such as IDE or neprilysine, appeared greatly increased in treated SAMP8 with higher protein levels of IDE than in control animals and consequently with substantially decreased βCTF protein levels. The results of the behavioural and biochemical studies in SAMP8 mice suggest that compound **23** acts centrally on 11β-HSD1.

Overall, behavioural tests and biochemical analyses confirmed a neuroprotective action of compound **23**, probably by reduction of inflammation and oxidative stress, as measured by reduction of IL-6 and iNOS.
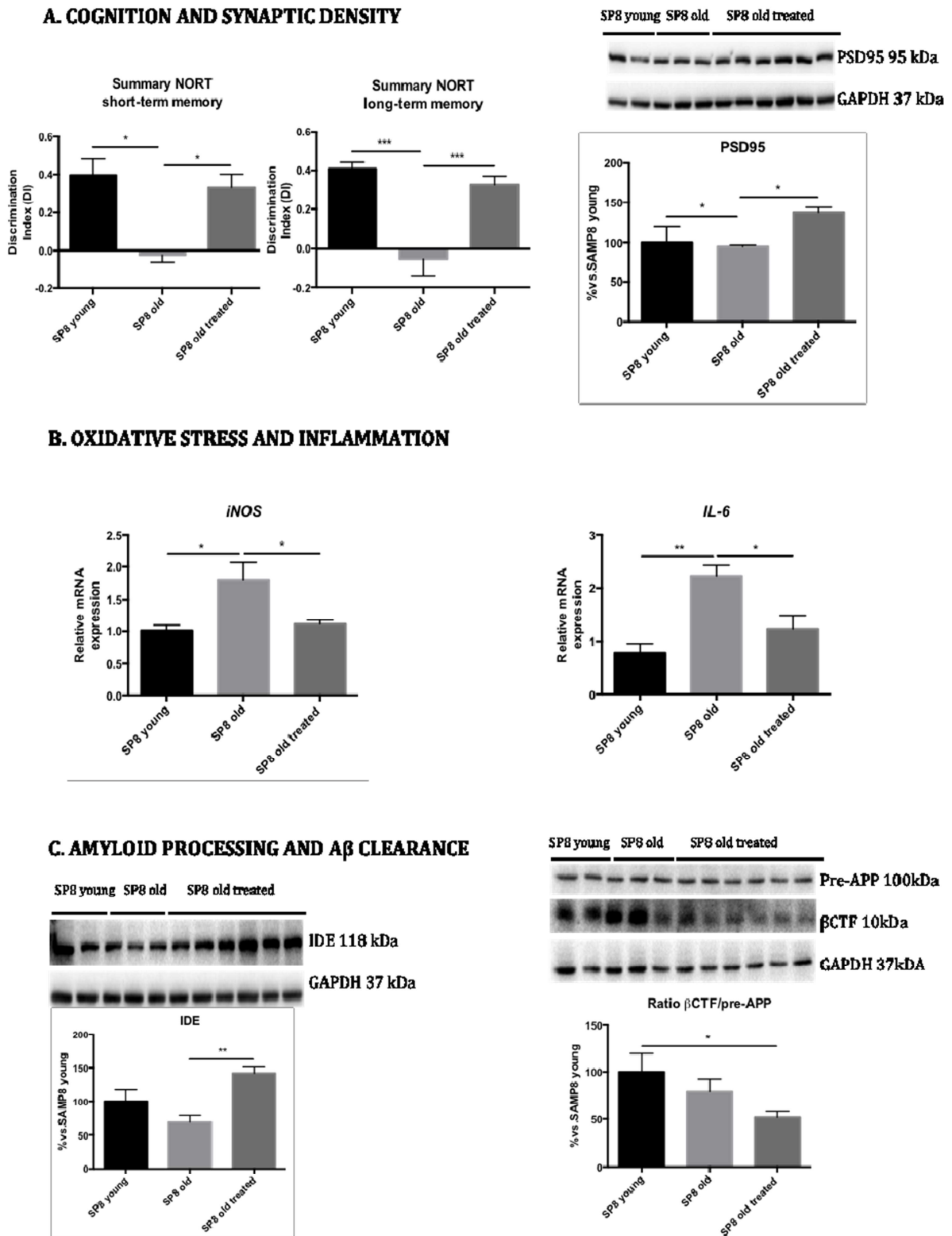
Figure 5. Results of *in vivo* **study. 2A. -Cognition and synaptic density: -Left panel:** Results. Discrimination index of Novel Object recognition test (NORT) obtained in

young SAMP8, old SAMP8 and treated SAMP8, at 2 and 24 h. -**Right Panel**: Representative Western blot (wb) for PSD95 and quantification. **2B. -Oxidative stress and inflammation: -Left Panel:** Oxidative stress gene expression iNOS. -**Right panel:** pro-inflammatory gene expression for IL-6. Gene exprexion levels were determined by real-time PCR. **2C. -Amyloid processing and β-CTF clearance: -Left panel:** Representative Western blot (wb) for IDE and quantification. **-Right panel:** Representative Western blot (wb) for Pre-APP and β-CTF and β-CTF/APP ratio quantification. For Western blot, bars represent mean ± standard error of the mean (SEM), and values are adjusted to 100% for levels SAMP8 young. For real-time PCR, mean ± SEM from five independent experiments performed in triplicate are represented. The One-Way ANOVA analysis and Tukey post hoc analysis were conducted. Statistical outliers (Grubbs' test) were removed from the analyses. $p < 0.05$; $p < 0.01$; $p < 0.001$.

5. Conclusions

We have found that adamantyl, widely used as a lipophilic substituent in 11β-HSD1 inhibitors, may successfully be replaced by other polycyclic hydrocarbons. The previously scarcely explored pyrrolidine-based polycyclic substituents presented here led to potent 11β-HSD1 inhibitors, and potentially these aliphatic ring-systems can serve as alternatives to adamantyl. Of note, the novel nanomolar inhibitors reported are achiral and easily synthesized in maximum four synthetic steps (compounds **19**, **21** and **23**) from commercially available starting materials. Biological profiling allowed us to select amide **23** for the first *in vivo* study in SAMP8 aiming to investigate the pharmacological effects of 11β-HSD1 inhibition in this model of cognitive dysfunction. In this study, prevention of cognitive impairment in aged SAMP8 after four-week treatment with **23** was demonstrated in comparison with control animals. The results provide further support for the neuroprotective effect of 11β-HSD1 inhibition, through reduction of neuroinflammation and oxidative stress, in cognitive decline related to the aging process. Due to the promising biological activity of **23**, further optimization is currently being carried out, with focus on modifying the RHS of the molecule to improve the selectivity and DMPK properties.

6. Experimental section

6.1. Chemistry

6.1.1. General

Melting points were determined in open capillary tubes with a MFB 595010M Gallenkamp. 400 MHz ^{1}H/100.6 MHz ^{13}C NMR spectra, and 500 MHz ^{1}H NMR spectra were recorded on Varian Mercury 400, and Varian Inova 500 spectrometers, respectively. The chemical shifts are reported in ppm (δ scale) relative to internal tetramethylsilane, and coupling constants are reported in Hertz (Hz). Assignments given for the NMR spectra of the new compounds have been carried out on the basis of DEPT, COSY ^{1}H/^{1}H (standard procedures), and COSY ^{1}H/^{13}C (gHSQC and gHMBC sequences) experiments. IR spectra were run on Perkin-Elmer Spectrum RX I spectrophotometer. Absorption values are expressed as wave-numbers (cm^{-1}); only significant absorption bands are given. Column chromatography was performed either on silica gel 60 Å (35−70 mesh) or on aluminium oxide, neutral, 60 Å (50-200 μm, Brockmann I). Thin-layer chromatography was performed with aluminum-backed

sheets with silica gel 60 F$_{254}$ (Merck, ref 1.05554), and spots were visualized with UV light and 1% aqueous solution of KMnO$_4$. The analytical samples of all of the new compounds which were subjected to pharmacological evaluation possessed purity ≥95% as evidenced by their elemental analyses.

6.1.2. General procedures for the synthesis of the compounds

6.1.2.1. General procedure A.

A solution of cyclohexane acyl chloride (1.2 mmol) in anhydrous acetone was added to a solution of the amine hydrochloride (1 mmol) and triethylamine (2 mmol) in anhydrous acetone. The reaction mixture was stirred at 90º C for 3 h. The resulting residue was dissolved with DCM (20 mL) and washed with 1 M aqueous solution of HCl (4 x 25 mL), dried over anh. Na$_2$SO$_4$ and filtered. The evaporation *in vacuo* of the organics gave the desired product.

6.1.2.2. General procedure B.

To a solution of the amine hydrochloride (1 mmol) in DCM (10 mL) were added 1-piperidinecarbonyl chloride (1.5 mmol) and triethylamine (4 mmol). The reaction mixture was stirred at rt overnight. To the resulting mixture was added saturated aqueous solution of NaHCO$_3$ (10 mL) and the phases were separated. The aqueous layer was extracted with further DCM (2 x 10 mL). The organics were washed with 10% Na$_2$CO$_3$ solution (30 mL), dried over anh. Na$_2$SO$_4$, filtered and concentrated *in vacuo* to give the desired product.

6.1.2.3. General procedure C.

To a solution of amine hydrochloride (1.1 mmol) in EtOAc (15 mL) were added the carboxylic acid (1 mmol), HOBt (1.5 mmol), EDC (1.5 mmol) and triethylamine (4 mmol) and the reaction mixture was stirred at rt overnight. To the resulting suspension was then added water (15 mL) and the phases were separated. The organic phase was washed with saturated aqueous NaHCO$_3$ solution (15 mL) and brine (15 mL), dried over anh. Na$_2$SO$_4$ and filtered. The organic layer was concentrated *in vacuo* to give the desired product.

6.1.2.4. General procedure D.

A solution or suspension of the amide or urea (1 mmol) and 5 wt. % palladium on carbon (50% in water, 10% of the weight) in absolute ethanol (ca 30 mL) was stirred at rt and atmospheric pressure under hydrogen for 3-72 h. The suspension was then

filtered and the solids were washed with EtOH (10 mL). The solvents were removed *in vacuo* to give the desired reduced product.

6.1.3. N-[Pentacyclo[6.4.0.0^{2,10}.0^{3,7}.0^{4,9}]dodec-8-yl] cyclohexanecarboxamide, (6).

From cyclohexane acyl chloride (128 mg, 0.88 mmol) in anhydrous acetone (0.6 mL) and amine **4** [38] (152 mg, 0.72 mmol) and triethylamine (0.25 mL, 1.74 mmol) in anhydrous acetone (0.9 mL) and following the general procedure A, amide **6** (215 mg, 95% yield) was obtained as a yellow solid. The analytical sample was obtained by crystallization from EtOAc / pentane (164 mg), mp 228−229 ºC; IR (ATR) ν: 580, 591, 604, 638, 663, 695, 722, 761, 824, 894, 933, 1143, 1194, 1221, 1277, 1304, 1336, 1386, 1448, 1547, 1639, 2851, 2923, 3271 cm^{-1}; ^{1}H-NMR (400 MHz, CDCl$_3$) δ: 1.08 (t, J = 2.8 Hz, 1 H, 9'-H), 1.18-1.34 [complex signal, 3 H, 3(5)-H$_{ax}$ and 4-H$_{ax}$], 1.39-1.55 [complex signal, 10 H, 5'(11')-H$_2$, 6'(12')-H$_2$ and 2(6)-H$_{ax}$], 1.66 (m, 1 H, 4-H$_{eq}$), 1.79 [m, 2 H, 3(5)-H$_{eq}$], 1.85 [m, 2 H, 2(6)-H$_{eq}$], 2.08 (tt, J = 11.6 Hz, J' = 3.4 Hz, 1 H, 1-H), 2.13 [b. s., 2 H, 4'(10')-H], 2.21 [m, 2 H, 2'(3')-H], 2.81 [b. s., 2 H, 1'(7')-H], 5.47 (s, 1 H, NH); ^{13}C-NMR (100.5 MHz, CDCl$_3$) δ: 21.5 [CH$_2$, C5'(C11')], 24.4 [CH$_2$, C6'(C12')], 25.7 (CH$_2$, C4), 25.8 [CH$_2$, C3(5)], 30.1 [CH$_2$, C2(C6)], 45.8 (CH, C1), 46.9 [CH, C2'(3')], 52.8 [CH, C4'(10')], 53.4 [CH, C1'(7')], 54.8 (CH, C9'), 65.4 (C, C8'), 176.7 (C, CO). Anal. Calcd for C$_{19}$H$_{27}$NO: C 79.95, H 9.54, N 4.91. Found: C 79.73, H 9.75, N 4.82.

6.1.4. N-[[Pentacyclo[6.4.0.0^{2,10}.0^{3,7}.0^{4,9}]dodec-8-yl]methyl]cyclohexanecarboxamide, (7).

From cyclohexane acyl chloride (119 mg, 0.81 mmol) in anhydrous acetone (0.6 mL) and amine **5** [38] (150 mg, 0.67 mmol) and triethylamine (0.23 mL, 1.62 mmol) in anhydrous acetone (0.8 mL) and following the general procedure A, amide **7** (155 mg, 78% yield) was obtained as a dark solid. The analytical sample was obtained by crystallization from EtOAc / pentane (77 mg), mp 148−149 ºC; IR (ATR) ν: 576, 589, 604, 621, 660, 672, 711, 800, 894, 956, 979, 1037, 1106, 1123, 1180, 1213, 1252, 1298, 1314, 1380, 1435, 1443, 1550, 1633, 1659, 2855, 2928, 3299 cm^{-1}; ^{1}H-NMR (400 MHz, CDCl$_3$) δ: 1.05 (b. s., 1 H, 9'-H), 1.17-1.33 [complex signal, 3 H, 3(5)-H$_{ax}$ and 4-H$_{ax}$], 1.35-1.55 [complex signal, 8 H, 5'(11')-H$_{exo\ or\ endo}$, 6'(12')-H$_2$ and 2(6)-H$_{ax}$], 1.56-1.70 [complex signal, 3 H, 5'(11')-H$_{endo\ or\ exo}$ and 4-H$_{eq}$], 1.74-1.87 [complex signal, 4 H, 2(6)-H$_{eq}$ and 3(5)-H$_{eq}$], 1.98 [b. s., 2 H, 4'(10')-H], 2.05 (tt, J = 11.6 Hz, J' = 3.2 Hz, 1

H, 1-H), 2.13 [b. s., 2 H, 1'(7')-H], 2.22 [m, 2 H, 2'(3')-H], 3.38 [d, J = 5.6 Hz, 2 H, NC$\underline{H}_2$], 5.20 [b. s., 1H, NH]; ^{13}C-NMR (100.5 MHz, CDCl$_3$) δ: 22.3 [CH$_2$, C5'(C11')], 24.2 [CH$_2$, C6'(12')], 25.7 (3 CH$_2$, C3, C4 and C5), 29.8 [CH$_2$, C2(6)], 36.9 (CH$_2$, $\underline{N}$CH$_2$), 42.7 (C, C8'), 45.7 (CH, C1), 47.9 [CH, C2'(3')], 51.2 (CH, C9'), 53.1 [CH, C1'(7')], 53.5 [CH, C4'(10')], 175.6 (C, CO). Anal. Calcd for C$_{20}$H$_{29}$NO·0.15 EtOAc: C 79.13, H 9.74, N 4.48. Found: C 79.03, H 9.88, N 4.52.

6.1.5. *N-[Pentacyclo[6.4.0.0^{2,10}.0^{3,7}.0^{4,9}]dodec-8-yl]piperidine-1-carboxamide, (8)*.

From amine **4** [38] (100 mg, 0.47 mmol), 1-piperidinecarbonyl chloride (0.09 mL, 0.71 mmol) and triethylamine (0.23 mL, 1.88 mmol) in DCM (5 mL) and following the general procedure B, amide **8** (72 mg, 54% yield) was obtained as a white solid. The analytical sample was obtained by crystallization from hot EtOAc (22 mg), mp 225−226 ºC; IR (ATR) ν: 700, 721, 734, 764, 794, 851, 866, 907, 954, 971, 1003, 1019, 1050, 1128, 1141, 1187, 1232, 1254, 1261, 1276, 1306, 1325, 1357, 1395, 1440, 1479, 1520, 1615, 2024, 2158, 2855, 2930, 3362 cm^{-1}; ^{1}H-NMR (400 MHz, CDCl$_3$) δ: 0.99 (broad s, 1 H, 9'-H), 1.43-1.65 complex signal, 14 H, 5'(11')-H$_2$, 6'(12')-H$_2$, 3(5)-H$_2$ and 4-H$_2$], 2.13 [broad s, 2 H, 4'(10')-H], 2.21 [broad s, 2 H, 2'(3')-H], 2.78 [broad s, 2 H, 1'(7')-H], 3.31 [m, 4 H, 2(6)-H$_2$], 4.53 (broad s, 1 H, NH); ^{13}C-NMR (100.5 MHz, CDCl$_3$) δ: 21.5 [CH$_2$, C5'(11')], 24.5 (CH$_2$, C4), 24.6 [CH$_2$, C6'(12')], 25.6 [CH$_2$, C3(5)], 45.2 [CH$_2$, C2(6)], 46.8 [CH, C2'(3')], 52.8 [CH, C4'(10')], 53.6 [CH, C1'(7')], 55.4 (CH, C9'), 65.8 (C, C8'), 157.4 (C, CO); HRMS-ESI+ m/z [*M*+H]$^+$ calcd for [C$_{18}$H$_{26}$N$_2$O+H]$^+$: 287.2118, found: 287.2118.

6.1.6. *N-[[Pentacyclo[6.4.0.0^{2,10}.0^{3,7}.0^{4,9}]dodec-8-yl]methyl]piperidine-1-carboxamide, (9)*.

From amine **5** [38] (96 mg, 0.42 mmol), 1-piperidinecarbonyl chloride (0.08 mL, 0.63 mmol) and triethylamine (0.21 mL, 1.68 mmol) in DCM (5 mL) and following the general procedure B, amide **9** (125 mg, quantitative yield) was obtained as a white solid. The analytical sample was obtained by crystallization from hot EtOAc (25 mg), mp 144−145 ºC; IR (ATR) ν: 554, 572, 623, 637, 678, 734, 763, 851, 869, 900, 908, 945, 969, 992, 1023, 1107, 1155, 1232, 1253, 1261, 1340, 1397, 1438, 1451, 1475, 1524, 1614, 2018, 2158, 2842, 2860, 2930, 3378 cm^{-1}; ^{1}H-NMR (400 MHz, CDCl$_3$) δ: 1.06 (broad s, 1 H, 9'-H), 1.40-1.70 [complex signal, 14 H, 5'(11')-H$_2$, 6'(12')-H$_2$, 3(5)-H$_2$ and 4-H$_2$], 2.00 [broad s, 2 H, 4'(10')], 2.13 [broad s, 2 H, 1'(7')-H], 2.22 [broad s, 2 H, 2'(3')-H], 3.28 [m, 4 H, 2(6)-H$_2$], 3.37 (d, J = 5.2 Hz, 2 H, NC$\underline{H}_2$), 4.18 (broad s, 1H, NH); ^{13}C-

NMR (100.5 MHz, CDCl$_3$) δ: 22.4 [CH$_2$, C5'(11')], 24.3 [CH$_2$, C6'(12')], 24.4 (CH$_2$, C4), 25.6 [CH$_2$, C3(5)], 38.6 (CH$_2$, $\underline{N}$CH$_2$), 44.5 (C, C8'), 45.0 [CH$_2$, C2(6)], 47.9 [CH, C2'(3')], 51.2 (CH, C9'), 53.1 [CH, C1'(7')], 53.6 [CH, C4'(10')], 157.8 (C, CO); HRMS-ESI+ m/z [M+H]$^+$ calcd for [C$_{19}$H$_{29}$N$_2$O+H]$^+$: 301.2274, found: 301.2276.

6.1.7. *(3-Azahexacyclo[7.6.0.0^{1,5}.0^{5,12}.0^{6,10}.0^{11,15}]pentadeca-7,13-dien-3-yl)(cyclohexyl) methanone, (11).*

From amine **10** [38] (400 mg, 2.03 mmol), cyclohexanecarboxylic acid (237 mg, 1.85 mmol), HOBt (375 mg, 2.78 mmol), EDC (430 mg, 2.78 mmol) and triethylamine (0.570 mL, 4.07 mmol) in ethyl acetate (30 mL) and following the general procedure C, an orange oil (627 mg) was obtained. Column chromatography (Al$_2$O$_3$, DCM/methanol) gave amide **11** (260 mg, 42% yield) as a white solid. The analytical sample was obtained by crystallization from *tert*-butanol, mp 111−113 ºC; IR (ATR) ν: 2961, 2930, 2853, 1630, 1443, 1425, 1347, 1305, 1223, 1194, 1138, 1067, 998, 897, 878, 830, 780, 749, 734, 696, 659, 646 cm^{-1}; ^{1}H-NMR (500 MHz, CDCl$_3$) δ: 1.17-1.24 [complex signal, 3 H, 4'-H$_{ax}$, 3'(5')-H$_{ax}$], 1.43 [complex signal, 2 H, 2'(6')-H$_{ax}$], 1.60-1.66 [complex signal, 3 H, 2'(6')-H$_{eq}$, 4'-H$_{eq}$], 1.75-1.78 [complex signal, 2 H, 3'(5')-H$_{eq}$], 2.13 (tt, J = 12.0 Hz, J' = 3.5 Hz, 1 H, 1'-H), 2.67 [m, 2 H, 10(11)-H], 2.98 [complex signal, 4 H, 6(12)-H, 9(15)-H], 3.18 (s, 2 H, 2-H$_2$ or 4-H$_2$), 3.19 (s, 2 H, 4-H$_2$ or 2-H$_2$), 6.00 [ddd, J = 6 Hz, J' = 3 Hz, J'' = 1.5 Hz, 2 H, 7(13)-H or 8(14)-H], 6.04 [ddd, J = 6 Hz, J' = 3 Hz, J'' = 1 Hz, 2 H, 8(14)-H or 7(13)-H]; ^{13}C-NMR (125.7 MHz, CDCl$_3$) δ: 25.8 (CH$_2$, C4'), 25.9 [CH$_2$, C3'(5')], 28.7 [CH$_2$, C2'(6')], 42.5 (CH, C1'), 45.5 (CH$_2$, C2 or C4), 46.7 (CH$_2$, C4 or C2), 62.0 [CH, C6(12) and C9(15)], 62.8 [CH, C10(11)], 69.1 (C, C1 or C5), 70.8 (C, C5 or C1), 132.8 [CH, C7(13) or 8(14)], 134.1 [CH, C8(14) or C7(13)], 174.4 (C, CO); MS (EI), (rt = 25.4 min), *m/z* (%); significant ions: 308 (20), 307 (M$^{+\bullet}$, 83), 252 (16), 242 (25), 198 (17), 197 (100), 196 [(C$_{14}$H$_{14}$N)$^+$, 39], 182 (19), 181 (15), 180 (41), 179 (16), 168 (24), 167 (25), 166 (15), 165 (38), 156 (21), 153 (23), 152 (27), 132 (64), 131 (100), 130 (64), 128 (17), 118 (19), 117 (19), 115 (23), 91 (18), 83 [(C$_6$H$_{11}$)$^+$, 85], 77 (15), 55 (72); HRMS-ESI+ m/z [M+H]$^+$ calcd for [C$_{21}$H$_{25}$NO+H]$^+$: 308.2009, found: 308.2003.

6.1.8. *(3-Azahexacyclo[7.6.0.0^{1,5}.0^{5,12}.0^{6,10}.0^{11,15}]pentadecane-3-yl)(cyclohexyl) methanone, (12).*

From amide **11** (118 mg, 0.40 mmol) and Pd/C (13 mg) and following the general procedure D (5 h), amide **12** (94 mg, 78% yield) was obtained as a white solid. The

analytical sample was obtained by crystallization from DCM/diethyl ether, mp 134−135 ºC; IR (ATR) ν: 2932, 2851, 1621, 1463, 1426, 1357, 1286, 1202, 1120, 1104, 1036, 1013, 969, 925, 886, 860, 825, 768, 732, 702, 657, 627 cm^{-1}; ^{1}H-NMR (500 MHz, CDCl$_3$) δ: 1.25 [complex signal, 3 H, 4'-H$_{ax}$, 3'(5')-H$_{ax}$], 1.48-1.57 [complex signal, 10 H, 7(13)-H$_2$, 8(14)-H$_2$, 17(21)-H$_{ax}$], 1.68 (m, 1 H, 4'-H$_{eq}$), 1.75-1.82 [complex signal, 4 H, 2'(6')-H$_{eq}$, 3'(5')-H$_{eq}$], 2.08 (broad signal, 4 H, 6(12)-H, 9(15)-H], 2.36 (tt, J = 12 Hz, J' = 3.5 Hz, 1 H, 1'-H), 2.41 [m, 2 H, 10(11)-H], 3.29 [s, 4 H, 2(4)-H$_2$]; ^{13}C-NMR (125.7 MHz, CDCl$_3$) δ: 21.5 [CH$_2$, C7(13) or C8(14)], 21.8 [CH$_2$, C8(14) or C7(13)], 25.8 (CH$_2$, C4'), 25.9 [CH$_2$, C3'(5')], 29.0 [CH$_2$, C2'(6')], 40.7 (CH$_2$, C2 or C4), 42.0 (CH$_2$, C4 or C2), 42.9 (CH, C1'), 49.6 [CH, C10(11)], 55.0 [CH, C6(12) or C9(15)], 55.1 [CH, C9(15) or C6(12)], 57.5 (C, C1 or C5], 59.3 (C, C5 or C1], 175.1 (C, CO); MS (EI), (rt = 26.7 min), m/z (%); significant ions: 312 (23), 311 (M$^{·+}$, 100), 270 (14), 257 (19), 256 (99), 243 (12), 228 [(C$_{15}$H$_{18}$NO)$^+$ 13], 202 (12), 201 (30), 184 (29), 129 (15), 128 (15), 91 (16), 83 [(C$_6$H$_{11}$)$^+$, 24], 55 (25). Anal. Calcd for C$_{21}$H$_{29}$NO: C 80.98, H 9.39, N 4.50. Found: 80.76, H 9.61, N 4.33.

6.1.9. *(3-Azahexacyclo[7.6.0.0^{1,5}.0^{5,12}.0^{6,10}.0^{11,15}]pentadeca-7,13-diene-3-yl)(piperidin-1-yl)methanone, (13)*.

From amine **10** [38] (400 mg, 2.03 mmol), 1-piperidinecarbonyl chloride (0.26 mL, 2.13 mmol) and triethylamine (0.56 mL, 4.06 mmol) in DCM and following the general procedure B amide **13** (443 mg, 71% yield) was obtained as a clear oil. Several attempts to crystallize this product met with failure. The product was used in the next step without further purification or characterization; MS (EI), (rt = 24.2 min), m/z (%); significant ions: 308 (M$^{·+}$, 46), 196 [(C$_{14}$H$_{14}$N)$^+$, 17], 165 (14), 130 (15), 112 [(C$_6$H$_{10}$NO)$^+$, 100], 84 [(C$_5$H$_{10}$N)$^+$, 17], 69 (41).

6.1.10. *(3-Azahexacyclo[7.6.0.0^{1,5}.0^{5,12}.0^{6,10}.0^{11,15}]pentadeca-3-yl)(piperidin-1-yl) methanone, (14)*.

From urea **13** (235 mg, 0.76 mmol) and Pd/C (24 mg) and following the general procedure D (3 h), urea **14** (171 mg, 72% yield) was obtained as a white solid, mp 124−126 ºC; IR (ATR) ν: 3457, 3291, 2936, 2867, 2839, 1615, 1538, 1461, 1415, 1370, 1332, 1304, 1252, 1226, 1202, 1159, 1124, 1110, 1027, 991, 915, 882, 851, 767, 722, 632 cm^{-1}; ^{1}H-NMR (500 MHz, CDCl$_3$) δ: 1.47-1.58 [complex signal, 14 H, 7(8,13,14)-H$_2$, 3'(5')-H$_2$, 4'-H$_2$], 2.05 [m, 4 H, 6(9,12,15)-H], 2.38 [m, 2 H, 10(11)-H], 3.19 [m, 8 H, 2(4)-H$_2$, 2'(6')-H$_2$]; ^{13}C-NMR (125.7 MHz, CDCl$_3$) δ: 21.7 [CH$_2$, C7(8, 13, 14)],

24.8 (CH$_2$, C4'), 25.9 [CH$_2$, C3'(5')], 43.3 [CH$_2$, C2(4)], 47.8 [CH$_2$, C16(20)], 49.6 [CH, C10(11)], 54.8 [CH, C6(9, 12, 15)], 58.8 [C, C1(5)], 163.3 (C, CO); MS (EI), (rt = 25.1 min), *m/z* (%); significant ions: 312 (M$^{\cdot+}$, 100), 201 (15), 200 [(C$_{14}$H$_{18}$N)$^+$, 82], 184 (33), 129 (36), 112 [(C$_6$H$_{10}$NO)$^+$, 54], 91 (16), 84 [(C$_5$H$_{10}$N)$^+$, 59], 69 (28). Anal. Calcd for C$_{20}$H$_{28}$N$_2$O: C 76.88, H 9.03, N 8.97. Found: 76.60, H 9.21, N 8.74.

6.1.11. *(4-Amino-3,5-dichlorophenyl)(3-azahexacyclo[7.6.0.0^{1,5}.0^{5,12}.0^{6,10}.0^{11,15}]pentadeca-7,13-dien-3-yl)methanone, (15).*

From amine **10** [38] (400 mg, 2.03 mmol), 4-amino-3,5-dichlorobenzoic acid (380 mg, 1.85 mmol), 1-hydroxybenzotriazole (HOBt) (375 mg, 2.78 mmol), 1-ethyl-3-(3-dimethylaminopropyl)carbodiimide (EDC) (430 mg, 2.78 mmol) and triethylamine (0.560 mL, 4.07 mmol) in EtOAc (30 mL) and DMF (2 mL) and following the general procedure C, a yellow solid (677 mg) was obtained. Column chromatography (Al$_2$O$_3$, DCM/methanol) furnished **15** (332 mg, 47% yield) as a white solid, mp 236−238 ºC; IR (ATR) ν: 3449, 3306, 3250, 3204, 2954, 2867, 2150, 1597, 1538, 1501, 1456, 1410, 1384, 1342, 1316, 1295, 1244, 1225, 1192, 1054, 1002, 943, 896, 875, 791, 745, 733, 686, 667, 643 cm^{-1}; ^{1}H-NMR (500 MHz, CDCl$_3$) δ: 2.61 [m, 2 H, 10(11)-H], 2.85 [broad s, 2 H, 6(12)-H or 9(15)-H], 2.94 [broad s, 2 H, 9(15)-H or 6(12)-H], 3.13 (broad s, 2 H, 2-H or 4-H), 3.33 (broad s, 2 H, 4-H or 2-H), 5.91 [m, 2 H, 7(13)-H or 8(14)-H], 6.03 [m, 2 H, 8(14)-H or 7(13)-H], 7.19 (s, 2 H, Ar-H); ^{13}C-NMR (125.7 MHz, CDCl$_3$) δ: 45.5 (CH$_2$, C2 or C4), 49.9 (CH$_2$, C4 or C2), 61.8 [CH, C6(12), C9(15)], 62.7 [CH, C10(11)], 68.8 (C, C1 or C5), 71.0 (C, C5 or C1), 118.7 (C, Ar-C$_{meta}$), 126.7 (C, C$_{ipso}$), 127.1 (CH, Ar-C$_{ortho}$), 132.9 [CH, C7(13) or 8(14)], 133.9 [CH, C8(14) or C7(13)], 141.3 (C, Ar-C$_{para}$), 166.8 (C, CO); GC/MS (EI), (rt = 30.7 min), *m/z* (%); significant ions: 388 [(C$_{21}$H$_{18}$^{37}Cl$_2$N$_2$O)$^{\cdot+}$, 2], 386 [(C$_{21}$H$_{18}$^{37}Cl^{35}ClN$_2$O)$^{\cdot+}$, 12], 384 [(C$_{21}$H$_{18}$^{35}Cl$_2$N$_2$O)$^{\cdot+}$, 18], 192 [(C$_7$H$_4$^{37}Cl$_2$NO)$^+$, 10], 190 [(C$_7$H$_4$^{37}Cl^{35}ClNO)$^+$, 63], 188 [(C$_7$H$_4$^{35}Cl$_2$NO)$^+$, 100], 180 (12), 160 (12), 124 (16); HRMS-ESI+ m/z [*M*+H]$^+$ calcd for [C$_{21}$H$_{18}$Cl$_2$N$_2$O+H]$^+$: 385.0869, found: 385.0875.

6.1.12. *(4-Amino-3,5-dichlorophenyl)   (3-azahexacyclo[7.6.0.0^{1,5}.0^{5,12}.0^{6,10}.0^{11,15}]pentadecan-3-yl)methanone, (16).*

From amide **15** (200 mg, 0.78 mmol) and Pd/C (24 mg) and following the general procedure D (5 h) a yellow solid (207 mg) was obtained. Column chromatography (Al$_2$O$_3$, DCM/methanol) gave the desired amide **16** (180 mg, 89% yield) as a white solid, mp 243−244 ºC; IR (ATR) ν: 3455, 3283, 3238, 3186, 2931, 2865, 1631, 1597,

1545, 1498, 1456, 1425, 1332, 1307, 1269, 1232, 1216, 1118, 1070, 1035, 944, 895, 789, 768, 745, 693, 647, 629 cm^{-1}; ^{1}H-NMR (500 MHz, CDCl$_3$) δ: 1.43-1.60 [complex signal, 8 H, 7(13)-H$_2$, 8(14)-H$_2$], 2.04 [broad s, 2 H, 6(12)-H or 9(15)-H], 2.12 [broad s, 2 H, 9(15)-H or 6(12)-H], 2.41 [m, 2 H, 10(11)-H], 3.29 (s, 2 H, 2-H$_2$ or 4-H$_2$), 3.53 (s, 2 H, 4-H$_2$ or 2-H$_2$), 7.40 (s, 2 H, Ar-H); ^{13}C-NMR (125.7 MHz, CDCl$_3$) δ: 21.5 [CH$_2$, C7(13) or C8(14)], 21.8 [CH$_2$, C8(14) or C7(13)], 40.8 (CH$_2$, C2 or C4), 45.5 (CH$_2$, C4 or C2), 49.6 [CH, C10(11)], 54.8 [broad CH, C6(12) and C9(15)], 57.9 (C, C1 or C5), 59.6 (C, C5 or C1), 118.8 (C, Ar-C$_{meta}$), 126.9 (C, C$_{ipso}$), 127.2 (CH, Ar-C$_{ortho}$), 141.4 (C, Ar-C$_{para}$), 167.0 (C, CO); MS (EI), (rt = 32.3 min), m/z (%); significant ions: 392 [(C$_{21}$H$_{22}$^{37}Cl$_2$N$_2$O)$^{+}$, 8], 390 [(C$_{21}$H$_{22}$^{37}Cl^{35}ClN$_2$O)$^{+}$, 42], 388 [(C$_{21}$H$_{22}$^{35}Cl$_2$N$_2$O)$^{+}$, 63], 200 (18), 192 [(C$_7$H$_4$^{37}Cl$_2$NO)$^{+}$, 11], 190 [(C$_7$H$_4$^{37}Cl^{35}ClNO)$^{+}$, 64], 188 [(C$_7$H$_4$^{35}Cl$_2$NO)$^{+}$, 100], 184 (33), 169 (13), 160 (12), 124 (13). Anal. Calcd for C$_{21}$H$_{22}$Cl$_2$N$_2$O·0.50H$_2$O: C 63.32, H 5.82, Cl 17.80, N 7.03. Found: C 63.23, H 5.71, Cl 17.82, N 6.77.

6.1.13. *(Cyclohexyl)(octahydro-2H-isoindol-2-yl)methanone, (**17**).*

From octahydro-1*H*-isoindole hydrochloride (300 mg, 2.40 mmol), cyclohexanecarboxylic acid (279 mg, 2.18 mmol), HOBt (442 mg, 3.27 mmol), EDC (506 mg, 3.27 mmol) and triethylamine (0.7 mL, 4.80 mmol) in EtOAc (10 mL) and following the general procedure C, **17** (458 mg, 89% yield) was obtained as a white solid. The analytical sample was obtained by crystallization from hot EtOAc (82 mg), mp 67 – 68 ºC; IR (ATR) ν: 734, 890, 973, 1073, 1113, 1136, 1173, 1184, 1307, 1341, 1358, 1443, 1481, 1622, 2851, 2873, 2917 cm^{-1}; ^{1}H-NMR (400 MHz, CDCl$_3$) δ: 1.16-1.30 (complex signal, 3 H, 3-H$_{ax}$, 4-H$_{ax}$ and 5-H$_{ax}$), 1.31-1.63 (complex signal, 10 H, 2-H$_{ax}$, 6-H$_{ax}$, 4'-H$_2$, 7'-H$_2$, 5'-H$_2$, 6'-H$_2$), 1.64-1.84 (complex signal, 5 H, 2-H$_{eq}$, 6-H$_{eq}$, 3-H$_{eq}$, 4-H$_{eq}$ and 5-H$_{eq}$), 2.16 (m, 1 H, 3a'-H or 7a'-H), 2.24 (m, 1 H, 7a'-H or 3a'-H), 2.30 [tt, J = 11.6 Hz, J' = 3.6 Hz, 1 H, 1-H], 3.31 (dd, J = 10.0 Hz, J' = 6.0 Hz, 1 H, 1'-H$_a$ or 3´-H$_a$), 3.36 (dd, J = 12.0 Hz, J' = 6.6 Hz, 1 H, 3'-H$_a$ or 1´-H$_a$), 3.40 (dd, J = 12.0 Hz, J' = 7.8 Hz, 1 H, 3'-H$_b$ or 1´-H$_b$), 3.45 (dd, J = 10.0 Hz, J' = 7.0 Hz, 1 H, 1'-H$_b$ or 3´-H$_b$); ^{13}C-NMR (100.5 MHz, CDCl$_3$) δ: 22.5 (CH$_2$, C5' or C6'), 22.8 (CH$_2$, C6' or C5'), 25.73 (CH$_2$), 25.78 (CH$_2$), 25.80 (CH$_2$), 25.84 (CH$_2$) and 25.91 (CH$_2$) [C4', C7', C3, C4 and C5], 28.8 (CH$_2$, C2 or C6), 29.0 (CH$_2$, C6 or C2), 35.8 (CH, C3a' or C7a'), 37.6 (CH, C7a' or C3a'), 42.7 (CH, C1), 49.3 (CH$_2$, C1' or C3'), 50.4 (CH$_2$, C3' or

C1'), 175.4 (C, CO). Anal. Calcd for $C_{15}H_{25}NO$: C 76.55, H 10.71, N 5.95. Found: 76.56, H 10.67, N 5.96.

6.1.14 *(4-Azatricyclo[5.2.1.0^{2,6}]dec-8-en-4-yl)(cyclohexyl)methanone, (**18**)*.

From 4-azatricyclo[5.2.1.0^{2,6}]dec-8-ene hydrochloride [58] (240 mg, 1.40 mmol), cyclohexanecarboxylic acid (163 mg, 1.27 mmol), HOBt (258 mg, 1.91 mmol), EDC (296 mg, 1.91 mmol) and triethylamine (0.8 mL, 5.59 mmol) in EtOAc (8 mL) and following the general procedure C, amide **18** (304 mg, 97% yield) was obtained as a yellowish solid. Column chromatography (hexane/EtOAc) gave **18** as a white solid (209 mg), mp 77−78 ºC; IR (ATR) ν: 702, 731, 761, 793, 897, 987, 1216, 1256, 1332, 1347, 1428, 1621, 2850, 2920 cm^{-1}; ^{1}H-NMR (400 MHz, CDCl$_3$) δ: 1.12-1.29 (complex signal, 3 H, 3-H$_{ax}$, 4-H$_{ax}$ and 5-H$_{ax}$), 1.36-1.51 (complex signal, 3 H, 2-H$_{ax}$, 6-H$_{ax}$ and 10'-H$_a$], 1.54 (dt, J = 8.4 Hz, J' = 1.6 Hz, 1 H, 10'-H$_b$), 1.60-1.70 [complex signal, 3 H, 2-H$_{eq}$, 6-H$_{eq}$ and 4-H$_{eq}$), 1.71-1.84 (complex signal, 2 H, 3-H$_{eq}$ and 5-H$_{eq}$), 2.16 (tt, J = 11.6 Hz, J' = 3.6 Hz, 1 H, 1-H), 2.82-3.00 (complex signal, 4 H, 1'-H, 7'-H, 2'-H and 6'-H), 3.10 (dd, J = 10.8 Hz, J' = 3.6 Hz, 1 H, 3'-H$_a$ or 5'- H$_a$), 3.21 (dd, J = 13.5 Hz, J' = 3.6 Hz, 1 H, 5'-H$_a$ or 3'- H$_a$), 3.29 (dd, J = 13.5 Hz, J' = 9.2 Hz, 1 H, 5'-H$_b$ or 3'- H$_b$), 3.43 (dd, J = 10.8 Hz, J' = 9.2 Hz, 1 H, 3'-H$_b$ or 5'- H$_b$), 6.14 (dd, J = 6.0 Hz, J' = 3.2 Hz, 1 H, 8'-H or 9'-H), 6.19 (dd, J = 6.0 Hz, J' = 3.2 Hz, 1 H, 9'-H or 8'-H); ^{13}C-NMR (100.5 MHz, CDCl$_3$) δ: 25.8 [CH$_2$, C3(5)], 25.9 (CH$_2$, C4), 28.69 (CH$_2$, C2 or C6), 28.71 (CH$_2$, C6 or C2), 42.7 (CH, C1), 43.8 (CH, C2' or C6'), 45.9 (CH, C6' or C2'), 46.66 (CH, C1' or C7'), 46.70 (CH, C7' or C1'), 48.0 (CH$_2$, C3' or C5'), 48.8 (CH$_2$, C5' or C3'), 51.9 (CH$_2$, C10'), 134.7 (CH, C8' or C9'), 136.1 (CH, C9' or C8'), 173.9 (C, CO). Anal. Calcd for $C_{16}H_{23}NO$: C 78.32, H 9.45, N 5.71. Found: 78.03, H 9.41, N 5.58.

6.1.15.*(4-Azatricyclo[5.2.1.0^{2,6}]dec-4-yl)(cyclohexyl)methanone, (**19**)*.

From amide **18** (177 mg) and Pd/C (36 mg) and following the general procedure D (18 h), amide **19** (156 mg, 88% yield) was obtained as a white solid, mp 83-84 ºC; IR (ATR) ν: 611, 625, 642, 886, 1002, 1133, 1170, 1187, 1204, 1218, 1290, 1327, 1344, 1357, 1425, 1446, 1623, 2871, 2936, 2945 cm^{-1}; ^{1}H-NMR (400 MHz, CDCl$_3$) δ: 1.20−1.94 (complex signal, 16 H, 3-H$_2$, 4-H$_2$, 5-H$_2$, 2-H$_2$, 6-H$_2$, 8'-H$_2$, 9'-H$_2$ and 10'-H$_2$), 2.18-2.27 (complex signal, 2 H, 1'-H and 7'-H), 2.37 (tt, J = 11.6 Hz, J' = 3.2 Hz, 1 H, 1-H), 2.52 (m, 1 H, 2'-H or 6'-H), 2.60 (m, 1 H, 6'-H or 2'-H), 3.03 (dd, J = 13.2 Hz, J' = 8.4 Hz, 1 H, 3'-H$_a$ or 5'- H$_a$), 3.26 (dd, J = 11.6 Hz, J' = 7.6 Hz, 1 H, 5'-H$_a$ or 3'- H$_a$),

3.57 (dd, J = 11.6 Hz, J' = 1.6 Hz, 1 H, 5'-H$_b$ or 3'- H$_b$), 3.84 (dd, J = 13.2 Hz, J' = 1.6 Hz, 1 H, 3'-H$_b$ or 5'- H$_b$); ^{13}C-NMR (100.5 MHz, CDCl$_3$) δ: 22.1 (CH$_2$, C8' or C9'), 22.8 (CH$_2$, C9' or C8'), 25.79 (CH$_2$), 25.86 (CH$_2$) and 25.88 (CH$_2$) (C3, C4 and C5), 28.87 (CH$_2$, C2 or C6), 28.89 (CH$_2$, C6 or C2), 41.2 (CH, C1' or C7'), 41.4 (CH, C7' or C1'), 42.0 (CH$_2$, C2' or C6'), 42.1 (CH$_2$, C10'), 42.9 (CH, C1), 44.0 (CH$_2$, C6' or C2'), 45.7 (CH$_2$, C3' or C5'), 46.9 (CH$_2$, C5' or C3'), 174.4 (C, CO). Anal. Calcd for C$_{16}$H$_{25}$NO: 77.68, H 10.19, N 5.66. Found: C 77.55, H 10.05, N 5.54.

6.1.16. *(4-Azatricyclo[5.2.2.0^{2,6}]undec-8-en-4-yl)(cyclohexyl)methanone, (**20**)*.

From 4-azatricyclo[5.2.2.0^{2,6}]undec-8-ene hydrochloride [59] (300 mg, 1.62 mmol), cyclohexanecarboxylic acid (188 mg, 1.47 mmol), HOBt (300 mg, 2.21 mmol), EDC (342 mg, 2.21 mmol) and triethylamine (0.9 mL, 6.47 mmol) in EtOAc (10 mL) and following the general procedure C, amide **20** (323 mg, 85% yield) was obtained as a yellowish solid. Column chromatography (hexane/EtOAc) gave **20** as a white solid (205 mg), mp 86−87 ºC; IR (ATR) ν: 703, 715, 849, 887, 986, 1044, 1132, 1165, 1216, 1239, 1307, 1347, 1357, 1375, 1431, 1625, 2850, 2921, 3037 cm^{-1}; ^{1}H-NMR (400 MHz, CDCl$_3$) δ: 1.15-1.34 (complex signal, 5 H, 10'-H$_a$, 11'-H$_a$, 3-H$_{ax}$, 4-H$_{ax}$ and 5-H$_{ax}$), 1.37-1.54 (complex signal, 4 H, 2-H$_{ax}$, 6-H$_{ax}$, 10'-H$_b$, 11'-H$_b$), 1.58-1.86 (complex signal, 5 H, 2-H$_{eq}$, 6-H$_{eq}$, 3-H$_{eq}$, 4-H$_{eq}$ and 5-H$_{eq}$), 2.23 (tt, J = 11.6 Hz, J' = 3.6 Hz, 1 H, 1-H), 2.42 (m, 1 H, 2'-H or 6'-H), 2.51-2.61 (complex signal, 3 H, 1'-H, 7'-H, 6'-H or 2'-H), 3.09 (d, J = 12.8 Hz, 1 H, 3'-H$_a$ or 5'-H$_a$), 3.11 (d, J = 12.4 Hz, 1 H, 5'-H$_a$ and 3'-H$_a$), 3.62 (dd, J = 12.4 Hz, J' = 9.2 Hz, 1 H, 5'-H$_b$ or 3'-H$_b$), 3.65 (dd, J = 12.8 Hz, J' = 9.6 Hz, 1 H, 3'-H$_b$ and 5'-H$_b$), 6.15-6.26 (complex signal, 2 H, 8'-H and 9'-H); ^{13}C-NMR (100.5 MHz, CDCl$_3$) δ: 24.2 (CH$_2$, C10' or C11'), 24.3 (CH$_2$, C11' or C10'), 25.81 (CH$_2$), 25.84 (CH$_2$) and 25.9 (CH$_2$) [C3, C4 and C5], 28.7 (CH$_2$, C2 or C6), 28.8 (CH$_2$, C6 or C2), 34.1 (CH, C1' and C7'), 41.9 (CH, C2' or C6'), 42.6 (CH, C1), 44.0 (CH, C6' or C2'), 50.8 (CH$_2$, C3' or C5'), 51.6 (CH$_2$, C5' or C3'), 132.9 (CH, C8' or C9'), 134.3 (CH, C9' or C8'), 173.9 (C, CO). Anal. Calcd for C$_{17}$H$_{25}$NO: C 78.72, 9.71, N 5.40. Found: C 78.82, H 9.71, N 5.30.

6.1.17. *(4-Azatricyclo[5.2.2.0^{2,6}]undec-4-yl)(cyclohexyl)methanone, (**21**)*.

From amide **20** (165 mg) and Pd/C (33 mg) and following the general procedure D (18 h) amide **21** (151 mg, 91% yield) was obtained as a white solid, mp 78−79 ºC; IR (ATR) ν: 622, 725, 868, 976, 1138, 1173, 1204, 1346, 1429, 1443, 1622, 2861, 2901, 2923 cm^{-1}; ^{1}H-NMR (400 MHz, CDCl$_3$) δ: 1.18-1.42 (complex signal, 5 H, 3-H$_{ax}$, 4-

H_{ax}, 5-H_{ax}, 8'-H_a and 9'-H_a), 1.44-1.90 (complex signal, 15 H, 3-H_{eq}, 4-H_{eq}, 5-H_{eq}, 2-H_2, 6-H_2, 1'-H, 7'-H, 8'-H_b, 9'-H_b, 10'-H_2 and 11'-H_2), 2.33 (m, 1 H, 2'-H or 6'-H), 2.37 (tt, J = 11.2 Hz, J' = 3.4 Hz, 1 H, 1-H), 2.43 (m, 1 H, 6'-H and 2'-H), 3.44-3.65 (complex signal, 4 H, 3'-H_2 and 5'-H_2); ^{13}C-NMR (100.5 MHz, CDCl$_3$) δ: 19.8 (CH$_2$, C9' or C8'), 20.1 (CH$_2$, C8' or C9'), 25.7 (CH, C1' and C7'), 25.81 (CH$_2$), 25.86 (CH$_2$) and 25.91 (CH$_2$) (C3, C4 and C5), 27.8 (CH$_2$, C11' or C10'), 28.0 (CH$_2$, C10' or C11'), 28.86 (CH$_2$, C2 or C6), 28.92 (CH$_2$, C6 or C2), 37.8 (CH$_2$, C2' or C6'), 40.0 (CH$_2$, C6' or C2'), 42.8 (CH, C1), 49.1 (CH$_2$, C3' or C5'), 49.9 (CH$_2$, C5' or C3'), 174.3 (C, CO). Anal. Calcd for C$_{17}$H$_{27}$NO: C 78.11, H 10.41, N 5.36. Found: C 78.14, H 10.35, N 5.14.

6.1.18. *(4-Azatetracyclo[5.3.2.0^{2,6}.0^{8,10}]dodec-11-en-4-yl)(cyclohexyl)methanone, (22)*.

From 4-azatetracyclo[5.3.2.0^{2,6}.0^{8,10}]dodec-11-ene hydrochloride [40] (2.06 g, 10.6 mmol), cyclohexanecarboxylic acid (1.24 g, 9.67 mmol), HOBt (1.96 g, 14.5 mmol), EDC (2.25 g, 14.5 mmol) and triethylamine (5.9 mL, 42.5 mmol) in EtOAc (150 mL) and following the general procedure C, amide **22** (2.43 g, 94% yield) was obtained as a yellowish solid. The analytical sample was obtained by crystallization from hot EtOAc (2.04 g), mp 96−97 ºC; IR (ATR) ν: 560, 570, 587, 696, 718, 741, 767, 812, 829, 847, 894, 915, 942, 963, 991, 1036, 1089, 1134, 1167, 1209, 1217, 1242, 1272, 1299, 1361, 1380, 1432, 1624, 2849, 2925, 3002, 3040 cm^{-1}; ^{1}H-NMR (400 MHz, CDCl$_3$) δ: 0.12-0.16 (complex signal, 2 H, 9'-H_2), 0.86-0.96 (complex signal, 2 H, 8'-H and 10'-H), 1.14-1.29 (complex signal, 3 H, 3-H_{ax}, 4-H_{ax} and 5-H_{ax}), 1.36-1.53 (complex signal, 2 H, 2-H_{ax} and 6-H_{ax}), 1.60-1.70 (complex signal, 3 H, 2-H_{eq}, 4-H_{eq} and 6-H_{eq}), 1.72-1.80 (complex signal, 2 H, 3-H_{eq} and 5-H_{eq}), 2.21 (tt, J = 11.6 Hz, J' = 3.4 Hz, 1 H, 1-H), 2.55 (dm, J = 12.8 Hz, 1 H, 2'-H or 6'-H), 2.67 (dm, J = 12.8 Hz, 1 H, 6'-H or 2'-H), 2.81-2.87 (complex signal, 2 H, 1'-H and 7'-H), 3.12 (dd, J = 11.0 Hz, J' = 5.0 Hz, 1 H, 3'-H_a or 5'-H_a), 3.15 (dd, J = 13.2 Hz, J' = 5.6 Hz, 1 H, 5'-H_a or 3'-H_a), 3.55 (t, J = 10.0 Hz, 1 H, 5'-H_b or 3'-H_b), 3.58 (t, J = 8.8 Hz, 1 H, 3'-H_b or 5'-H_b), 5.73 (ddd, J = 14.4 Hz, J' = 8.4 Hz, J'' = 2.0 Hz, 1 H, 11'-H or 12'-H], 5.77 (ddd, J = 14.4 Hz, J' = 8.4 Hz, J'' = 2.0 Hz, 1 H, 12'-H or 11'-H]; ^{13}C-NMR (100.5 MHz, CDCl$_3$) δ: 4.1 (CH$_2$, C9'), 10.0 (CH, C8' or C10'), 10.2 (CH, C10' or C8'), 25.80 (CH$_2$), 25.83 (CH$_2$) and 25.9 (CH$_2$) [C3, C4 and C5], 28.7 (CH$_2$, C2 or C6), 28.8 (CH$_2$, C6 or C2), 35.6 (CH, C1' or C7'), 35.7 (CH, 7' or C1'), 42.6, (CH, C1), 42.7 (CH, C2' or C6'), 44.8 (CH, C6' or C2'), 49.6 (CH$_2$, C3' or C5'), 50.6 (CH$_2$, C5' or C3'), 128.1 (CH, C11' or C12'), 129.6

(CH, C12' or C11'), 174.1 (C, CO). Anal. Calcd for $C_{18}H_{25}NO$: C 79.66, H 9.29, N 5.16. Found: C 79.64, H 9.24, N 5.21.

6.1.19. *(4-Azatetracyclo[5.3.2.0^{2,6}.0^{8,10}]dodec-4-yl)(cyclohexyl)methanone, (23).*

From **22** (500 mg) and Pd/C (100 mg) and following the general procedure D (72 h) amide **23** (426 mg, 83% yield) was obtained as a white solid, mp 74−75 ºC; IR (ATR) ν: 651, 679, 707, 729, 748, 789, 805, 826, 839, 865, 885, 950, 961, 988, 1016, 1030, 1082, 1113, 1133, 1171, 1205, 1213, 1234, 1264, 1295, 1325, 1346, 1358, 1427, 1471, 1486, 1623, 2846, 2897, 2928, 3009, cm^{-1}; ^{1}H-NMR (400 MHz, CDCl$_3$) δ: 0.45 (dt, J = 6.0 Hz, J' = 8.0 Hz, 1 H, 9'-H$_a$), 0.78 (m, J = 6.0 Hz, J' = 3.6 Hz, 1 H, 9'-H$_b$), 0.90-0.96 (complex signal, 2 H, 8'-H and 10'-H), 1.00-1.14 (complex signal, 2 H, 11'-H$_{ax}$ and 12'-H$_{ax}$), 1.17-1.34 [complex signal, 5 H, 11'-H$_{eq}$, 12'-H$_{eq}$, 3-H$_{ax}$, 4-H$_{ax}$ and 5-H$_{ax}$], 1.42-1.61 (complex signal, 2 H, 2-H$_{ax}$ and 6-H$_{ax}$), 1.67 (m, 1 H, 4'-H$_{eq}$), 1.69-1.83 (complex signal, 4 H, 3-H$_{eq}$, 4-H$_{eq}$, 5-H$_{eq}$, 6-H$_{eq}$), 1.84-1.91 (complex signal, 2 H, 1'-H and 7'-H), 2.38 [tt, J = 11.6 Hz, J' = 3.6 Hz, 1 H, 1-H], 2.50 (dm, J = 12.8 Hz, 1 H, 2'-H or 6'-H), 2.55 (dm, J = 12.8 Hz, 1 H, 6'-H or 2'-H), 3.32 (dd, J = 12.8 Hz, J' = 8.8 Hz, 1 H, 3'-H$_a$ or 5'-H$_a$), 3.52 (m, 2 H, 5'-H$_2$ or 3'-H$_2$), 3.76 (dd, J = 12.8 Hz, J' = 3.0 Hz, 1 H, 3'-H$_b$ or 5'-H$_b$); ^{13}C-NMR (100.5 MHz, CDCl$_3$) δ: 4.7 (CH$_2$, C9'), 14.9 (CH, C8' or C10'), 15.1 (CH, C10' or C8'), 17.3 (CH$_2$, C11' or C12'), 17.9 (CH$_2$, C12' or C11'), 25.8 (CH$_2$, C4), 25.9 [CH$_2$, C3(5)], 28.87 (CH$_2$, C2 or C6), 28.92 (CH$_2$, C6 or C2), 29.0 (CH, C1' or C7'), 29.4 (CH, C7' or C1'), 38.4 (CH, C2' or C6'), 40.5, (CH, C6' or C2'), 42.7 (CH, C1), 48.1 (CH, C3' or C5'), 49.3 (CH$_2$, C5' or C3'), 174.4 (C, CO). Anal. Calcd for $C_{18}H_{27}NO$: C 79.07, H 9.95, N 5.12. Found: 79.15, H 9.88, N 5.29.

6.1.20. *(4-Azatetracyclo[5.4.2.0^{2,6}.0^{8,11}]trideca-9,12-dien-4-yl)(cyclohexyl) methanone, (24).*

From 4-azatetracyclo[5.4.2.0^{2,6}.0^{8,11}]trideca-9,12-diene hydrochloride [40] (139 mg, 0.66 mmol), cyclohexanecarboxylic acid (77 mg, 0.60 mmol), HOBt (122 mg, 0.90 mmol), EDC (139 mg, 0.90 mmol) and triethylamine (0.4 mL, 2.64 mmol) in EtOAc (6 mL) and following the general procedure C, amide **24** (151 mg, 80% yield) was obtained as a yellowish solid. The analytical sample was obtained by crystallization from hot EtOAc (97 mg), mp 120−121 ºC; IR (ATR) ν: 730, 760 788, 808, 967, 994, 1173, 1187, 1214, 1235, 1294, 1361, 1442, 1463, 1617, 2860, 2901, 2922 cm^{-1}; ^{1}H-NMR (400 MHz, CDCl$_3$) δ: 1.15-1.30 [complex signal, 3 H, 3-H$_{ax}$, 4-H$_{ax}$ and 5-H$_{ax}$],

1.38-1.54 [complex signal, 2 H, 2-H_{ax} and 6-H_{ax}], 1.60-1.72 (complex signal, 3 H, 2-H_{eq}, 4-H_{eq} and 6-H_{eq}), 1.73-1.82 (complex signal, 2 H, 3-H_{eq} and 5-H_{eq}), 2.24 [tt, J = 11.6 Hz, J' = 3.6 Hz, 1 H, 1-H], 2.37 (tdd, J = 9.6 Hz, J' = 5.8 Hz, J'' = 2.8 Hz, 1 H, 2'-H or 6'-H), 2.50 (tdd, J = 8.8 Hz, J' = 5.6 Hz, J'' = 2.8 Hz, 1 H, 6'-H or 2'-H), 2.60-2.66 (complex signal, 2 H, 1'-H and 7'-H), 2.67-2.70 (complex signal, 2 H, 8'-H and 11'-H), 3.17-3.24 (complex signal, 2 H, 3'-H_a and 5'-H_a), 3.63-3.73 (complex signal, 2 H, 3'-H_b and 5'-H_b), 5.84-5.87 (complex signal, 2 H, 9'-H and 10'-H), 5.89-5.99 (complex signal, 2 H, 12'-H and 13'-H); ^{13}C-NMR (100.5 MHz, CDCl$_3$) δ: 25.81 (CH$_2$), 25.84 (CH$_2$) and 25.9 (CH$_2$) (C3, C4 and C5), 28.7 (CH$_2$, C2 or C6), 28.8 (CH$_2$, C6 or C2), 39.36 (CH, C1' or C7'), 39.37 (CH, C7' or C1'), 41.1 (CH, C2' or C6'), 42.6 (CH, C1), 43.2 (CH, C6' or C2'), 44.9 (CH, C8' or C11'), 45.1 (CH, C11' or C8'), 50.7 (CH$_2$, C3' or C5'), 51.5 (CH$_2$, C5' or C3'), 129.0 (CH, C12' or C13'), 130.3 (CH, C13' or C12'), 137.7 (CH, C9' or C10'), 138.0 (CH, C10' or C9'), 174.0 (C, CO). Anal. Calcd for C$_{19}$H$_{25}$NO: C 80.52, H 8.89, N 4.94. Found: 80.31, H 8.81, N 4.97.

6.1.21. *(4-Azatetracyclo[5.4.2.0^{2,6}.0^{8,11}]tridec-4-yl)(cyclohexyl)methanone, (**25**).*

From 4-azatetracyclo[5.4.2.0^{2,6}.0^{8,11}]tridecane hydrochloride [40] (235 mg, 1.10 mmol), cyclohexanecarboxylic acid (128 mg, 1.0 mmol), HOBt (203 mg, 1.50 mmol), EDC (232 mg, 1.50 mmol) and triethylamine (0.6 mL, 4.40 mmol) in EtOAc (10 mL) and following the general procedure C, amide **25** (253 mg, 80% yield) was obtained as a yellowish solid. The analytical sample was obtained by crystallization from hot EtOAc (110 mg), mp 115−116 ºC; IR (ATR) ν: 658, 731, 887, 988, 1133, 1172, 1204, 1236, 1357, 1434, 1440, 1621, 2908, 2925 cm^{-1}; ^{1}H-NMR (400 MHz, CDCl$_3$) δ: 1.18-1.34 (complex signal, 3 H, 3-H_{ax}, 4-H_{ax} and 5-H_{ax}), 1.42-1.62 (complex signal, 6 H, 1'-H, 7'-H, 2-H_{ax}, 6-H_{ax}, 12'-H_a and 13'-H_a), 1.64-1.92 (complex signal, 7 H, 2-H_{eq}, 6-H_{eq}, 3-H_{eq}, 4-H_{eq}, 5-H_{eq}, 12'-H_b and 13'-H_b), 2.02-2.20 (complex signal, 5 H, 2'-H or 6'-H, 9'-H_a, 9'-H_b, 10'-H_a and 10'-H_b), 2.27 (m, 1 H, 6'-H or 2'-H), 2.34-2.44 (complex signal, 3 H, 1-H, 8'-H and 11'-H), 3.48-3.70 (complex signal, 4 H, 3'-H_2 and 5'-H_2); ^{13}C-NMR (100.5 MHz, CDCl$_3$) δ: 15.0 (CH$_2$, C12' or C13'), 15.3 (CH$_2$, C13' or C12'), 20.8 [CH$_2$, C9'(10')], 25.82 (CH$_2$), 25.88 (CH$_2$) and 25.92 (CH$_2$) (C3, C4 and C5), 28.88 (CH$_2$, C2 or C6), 28.95 (CH$_2$, C6 or C2), 31.2 (CH, C1' or C7'), 31.5 (CH, C7' or C1'), 36.37 (CH, C8' or C11'), 36.44 (CH, C11' or C8'), 37.4 (CH, C2' or C6'), 39.5 (CH, C6' or C2'), 42.8 (CH, C1), 48.8 (CH$_2$, C3' or C5'), 49.7 (CH$_2$, C5' or C3'), 174.4 (C, CO).

Anal. Calcd for $C_{19}H_{29}NO$: C 79.39, H 10.17, N 4.87. Found: C 79.20, H 10.30, N 4.72.

6.1.22. *(12-Azatricyclo[4.4.3.0^{1,6}]trideca-3,8-dien-12-yl)(cyclohexyl)methanone, (26)*.

From 12-azatricyclo[4.4.3.0^{1,6}]trideca-3,8-diene hydrochloride [41] (150 mg, 0.71 mmol), cyclohexanecarboxylic acid (82 mg, 0.64 mmol), HOBt (131 mg, 0.97 mmol), EDC (150 mg, 0.97 mmol) and triethylamine (0.4 mL, 2.82 mmol) in EtOAc (6 mL) and following general procedure C, amide **26** (185 mg, 92% yield) was obtained as a yellowish solid. The analytical sample was obtained by crystallization from hot EtOAc (106 mg), mp 116−117 ºC; IR (ATR) ν: 605, 676, 739, 813, 865, 1004, 1187, 1207, 1224, 1332, 1347, 1427, 1629, 2858, 2918 cm^{-1}; ^{1}H-NMR (400 MHz, CDCl$_3$) δ: 1.16-1.31 (complex signal, 3 H, 3(5)-H$_{ax}$ and 4-H$_{ax}$), 1.51 [m, 2 H, 2(6)-H$_{ax}$], 1.62-1.84 [complex signal, 5 H, 2(6)-H$_{eq}$, 3(5)-H$_{eq}$ and 4-H$_{eq}$], 1.92-2.10 [complex signal, 8 H, 2'(10')-H$_2$ and 5'(7')-H$_2$], 2.29 [tt, J = 11.6 Hz, J' = 3.6 Hz, 1 H, 1-H], 3.35-3.37 (complex signal, 4 H, 3'-H$_a$, 3'-H$_b$, 5'-H$_a$ and 5'-H$_b$), 5.48-5.57 [complex signal, 4 H, 3'(9')-H and 4'(8')-H]; ^{13}C-NMR (100.5 MHz, CDCl$_3$) δ: 25.8 (CH$_2$, C4), 25.9 [CH$_2$, C3(5)], 28.9 [CH$_2$, C2(6)], 32.1 [CH$_2$, C2'(10') or C5'(7')], 32.2 [CH$_2$, C5'(7') or C2'(10')], 37.3 (C, C1' or C6'), 39.2 (C, C6' or C1'), 42.6 (CH, C1), 55.3 (CH$_2$, C11' or C13'), 56.1 (CH$_2$, C13' or C11'), 123.3 (CH, C3' and C9'), 123.9 (CH, C4' and C8'), 176.3 (C, CO); HRMS-ESI+ m/z [M+H]$^+$ calcd for [C$_{19}$H$_{27}$NO+H]$^+$: 286.2165, found: 286.2176.

6.1.23. *(12-Azatricyclo[4.4.3.0^{1,6}]tridec-12-yl)(cyclohexyl)methanone, (27)*.

From **26** (362 mg) and Pd/C (72 mg) and following the general procedure D (24 h), amide **27** (330 mg, 90% yield) was obtained as a white solid. The analytical sample was obtained by crystallization from hot EtOAc (178 mg), mp 160−161 ºC; IR (ATR) ν: 670, 764, 874, 891, 976, 1157, 1290, 1343, 1360, 1435, 1623, 1635, 2850, 2907, 2921 cm^{-1}; ^{1}H-NMR (400 MHz, CDCl$_3$) δ: 1.18-1.29 [complex signal, 3 H, 3(5)-H$_{ax}$ and 4-H$_{ax}$], 1.31-1.62 [complex signal, 18 H, 2`(6)-H$_{ax}$, 3'(9')-H$_2$, 4'(8')-H$_2$, 5'(7')-H$_2$, 10'(13')-H$_2$], 1.64-1.84 [complex signal, 5 H, 2(6)-H$_{eq}$, 3(5)-H$_{eq}$ and 4-H$_{eq}$], 2.30 [tt, J = 11.6 Hz, J' = 3.6 Hz, 1 H, 1-H], 2.70-3.90 (complex signal, 4 H, 3'-H$_2$ and 5'-H$_2$); ^{13}C-NMR (100.5 MHz, CDCl$_3$) δ: 21.6 [CH$_2$, C3'(9') or C4'(8')], 21.8 [CH$_2$, C4'(8') or C3'(9')], 25.8 (CH$_2$, C4), 25.9 [CH$_2$, C3(5)], 28.9 [CH$_2$, C2(6)], 39.8 (C, C1' and C6'), 41.7 [CH$_2$, C2'(10') and C5'(7')], 42.6 (CH, C1), 55.1 (CH$_2$, C11' or C13'), 55.8 (CH$_2$,

C13' or C11'), 176.0 (C, CO). Anal. Calcd for $C_{19}H_{31}NO$: C 78.84, H 10.80, N 4.84. Found: 78.83, H 10.74, N 4.75.

6.1.24.   *(3,4,8,9-Tetramethyl-12-azatricyclo[4.4.3.0^{1,6}]trideca-3,8-dien-12-yl) (cyclohexyl)methanone, (28).*

From 3,4,8,9-tetramethyl-12-azatricyclo[4.4.3.0^{1,6}]trideca-3,8-diene hydrochloride [41] (136 mg, 0.51 mmol), cyclohexanecarboxylic acid (62 mg, 0.48 mmol), HOBt (111 mg, 0.82 mmol), EDC (127 mg, 0.82 mmol) and triethylamine (0.3 mL, 2.38 mmol) in EtOAc (6 mL) and following the general procedure C, amide **28** (138 mg, 79% yield) was obtained as a yellowish solid. Column chromatography (hexane/EtOAc) gave **28** as a white solid (74 mg), mp 162−163 ºC; IR (ATR) ν: 748, 785, 848, 973, 1118, 1358, 1434, 1441, 1603, 1613, 2861, 2931 cm^{-1}; ^{1}H-NMR (400 MHz, CDCl$_3$) δ: 1.40-1.1.54 [complex signal, 3 H, 3(5)-H$_{ax}$ and 4-H$_{ax}$], 1.56 (s, 12 H, CH$_3$), 1.62-1.98 [complex signal, 15 H, 3(5)-H$_{eq}$, 4-H$_{eq}$, 2-H$_2$, 6-H$_2$, 2'(10')-H$_2$, 5'(7')-H$_2$], 2.28 (tt, 1 H, J = 11.6 Hz, J' = 3.2 Hz, 1 H, 1-H), 3.28-3.34 (complex signal, 4 H, 11'-H$_2$ and 13'-H$_2$); ^{13}C-NMR (100.5 MHz, CDCl$_3$) δ: 18.68 [CH$_3$, H$_3$<u>C</u>-C3'(9') or H$_3$<u>C</u>-C4'(8')], 18.71 [CH$_3$, H$_3$<u>C</u>-C4'(8') or H$_3$<u>C</u>-C3'(9')], 25.8 (CH$_2$, C4), 25.9 [CH$_2$, C3(5)], 28.9 [CH$_2$, C2(6)], 38.6 (CH$_2$, C1' or C6'), 38.7 [CH$_2$, C2'(10') or C5'(7')], 38.8 [CH$_2$, C5'(7') or C2'(10')], 40.4 (CH$_2$, C6' or C1'), 42.6 (CH, C1), 55.5 (CH$_2$, C11' or C13'), 56.4 (CH$_2$, C13' or C11'), 121.6 [C, C3'(9') or C4'(8')], 122.2 (C, C4'(8') or C3'(9')], 176.4 (C, CO); HRMS-ESI+ m/z [*M*+H]$^+$ calcd for [C$_{23}$H$_{36}$NO+H]$^+$: 342.2791, found: 342.2793.

6.1.25.   *(7,8,9,10-Tetramethyl-3-azapentacyclo[7.2.1.1^{5,8}.0^{1,5}.0^{7,10}]tridec-3-yl) (cyclohexyl) methanone*, (**29**).

From 7,8,9,10-tetramethyl-3-azapentacyclo[7.2.1.1^{5,8}.0^{1,5}.0^{7,10}]tridecane hydrochloride [40] (145 mg, 0.54 mmol), cyclohexanecarboxylic acid (67 mg, 0.52 mmol), HOBt (105 mg, 0.78 mmol), EDC (121 mg, 0.78 mmol) and triethylamine (0.3 mL, 2.29 mmol) in EtOAc (6 mL) and following the general procedure C, amide **29** (143 mg, 78% yield) was obtained as a yellowish solid. Column chromatography (hexane/EtOAc) gave **29** as a white solid (101 mg), mp 100−101 ºC; IR (ATR) ν: 636, 747, 791, 829, 866, 891, 977, 1026, 1083, 1124, 1207, 1243, 1266, 1346, 1382, 1442, 1625, 2857, 2925 cm^{-1}; ^{1}H-NMR (400 MHz, CDCl$_3$) δ: 0.84 [dd, J = 10.8 Hz, J' = 4.8 Hz, 4 H, 6'(13')-H$_2$ or 11'(12')-H$_2$], 0.93 (d, J = 3.6 Hz, 12 H, 7'(8')-C<u>H</u>$_3$ and 9'(10')-C<u>H</u>$_3$], 1.18-1.34 [complex signal, 3 H, 3(5)-H$_{ax}$ and 4-H$_{ax}$], 1.52 (m, 2 H, 2(6)-H$_{ax}$), 1.64-1.84 [complex signal, 9 H, 3(5)-H$_{eq}$, 4-H$_{eq}$, 2(6)-H$_{ax}$ and 11'(12')-H$_2$ or 6'(13')-H$_2$], 2.35 (tt, 1 H, J =

11.6 Hz, J' = 3.2 Hz, 1 H, 1-H), 3.59 (d, J = 15.6 Hz, 4 H, 2'-H$_2$ and 4'-H$_2$); ^{13}C-NMR (100.5 MHz, CDCl$_3$) δ: 15.5 [CH$_3$, H$_3$$\underline{C}$-C7'(8') or H$_3$$\underline{C}$-C9'(10')], 15.6 [CH$_3$, H$_3$$\underline{C}$-C9'(10') or H$_3$$\underline{C}$-C7'(8')], 25.8 (CH$_2$, C4), 25.9 [CH$_2$, C3(5)], 29.0 [CH$_2$, C2(6)], 42.4 (CH, C1), 42,9 [CH$_2$, C6'(13') or C11'(12')], 43.0 [CH$_2$, C11'(12') or C6'(13')], 45.3 [C, C7'(8') or C9'(10')], 45.4 [C, C9'(10') or C7'(8')], 47.0 (C, C1' or C5'), 48.9 (C, C5' or C1'), 51.6 [CH$_2$, C2' or C4'], 53.1 [CH$_2$, C4' or C2'], 174.6 (C, CO). Anal. Calcd for C$_{23}$H$_{35}$NO: C 80.88, H 10.33, N 4.10. Found: 80.97, H 10.27, N 4.00.

6.2. Molecular modeling

Docking calculations were carried out using Glide [60], with the X-ray structure of human enzyme 4BB6 [61]. The geometry of each ligand was energy minimized and the centroid of the inhibitor cocrystalised in 4BB6 was used to generate the docking cavity by selecting all the residues located within 20 Å from the ligand. Between 70 and 100 poses were generated for each ligand, and the best-scored poses (and the expected arrangement within the binding pocket) were chosen as starting structures for MD simulations.

For each ligand-protein complex two independent 50ns MD simulations were run to check the consistency of the binding mode. To this end, the ligand-protein complex was immersed in an octahedral box of TIP3P [62] water molecules and sodium ions were added to neutralize the system. The force field ff99SBildn [63-64] was used for the protein parameters, and RESP charges at the HF/6-31G (d) together with the gaff [65] force field were used to for the ligand and NADP parameters. All systems were refined using a three-step energy minimization procedure (involving first hydrogen atoms, then water molecules, and finally the whole system) and a six-step equilibration (heating the system from 0 K to 300 K in 6 steps of 20 ps, the first, 50 ps the next four, and 5 ns the last one).

6.3. Human 11β-HSD1 in vitro enzyme inhibition assay

11β-HSD1 activity was determined in mixed sex, human liver microsomes (Celsis In-vitro Technologies) by measuring the conversion of ^{3}H-cortisone to ^{3}H-cortisol. Percentage inhibition was determined relative to a no inhibitor control. 5 μg of human liver microsomes were pre-incubated at 37°C for 15 min with inhibitor and 1 mM NADPH in a final volume of 90 μL Krebs buffer. 10 μL of 200 nM ^{3}H-cortisone was then added followed by incubation at 37°C for a further 30 min. The assay was

terminated by rapid freezing on dry ice and ^{3}H-cortisone to ^{3}H-cortisol conversion determined in 50 µL of the defrosted reaction by capturing liberated ^{3}H-cortisol on anti-cortisol (HyTest Ltd)-coated scintillation proximity assay beads (protein A-coated YSi, GE Healthcare). A nanomolar 11β-HSD1 inhibitor, UE2316, was added as a positive control within in each set of assays. IC_{50} values for UE2316 were within the normal range across each test occasion [66].

6.4. Mouse 11β-HSD1 in vitro enzyme inhibition assay

11β-HSD1 activity was determined in pooled mouse (CD-1) liver microsomes (Celsis In-vitro Technologies) by measuring the conversion of cortisone to cortisol by LC/MS. Percentage inhibition was determined relative to a no inhibitor control. 5 µg of mouse liver microsomes were pre-incubated at 37°C for 15 min with inhibitor and 1 mM NADPH in a final volume of 90 µL Krebs buffer. 10 µL of 2 µM cortisone was then added followed by incubation at 37°C for a further 30 min. The assay was terminated by rapid freezing on dry ice and subsequent extraction with acetonitrile on thawing. Samples dried down under nitrogen at 65°C and solubilised in 100 µl 70:30 H_2O:ACN and removed to a 96-well V-bottomed plate for LC/MS analysis. Separation was carried out on a sunfire 150 x 2.1 mm, 3.5 µM column using a H_2O:ACN gradient profile. Typical retention times were 2.71 min for cortisol and 2.80 min for cortisone. The peak area was calculated and the concentration of each compound determined from the calibration curve.

6.5. Microsomal stability assay

The microsomal stability of each compound was determined using either human or mouse liver microsomes (Celsis In-vitro Technologies). Microsomes were thawed and diluted to a concentration of 2 mg/mL in 50 mM $NaPO_4$ buffer pH 7.4. Each compound was diluted in 4 mM NADPH (made in the phosphate buffer above) to a concentration of 10 µM. Two identical incubation plates were prepared to act as a 0 minute and a 30 minute time point assay. 30 µL of each compound dilution was added in duplicate to the wells of a U-bottom 96-well plate and warmed at 37°C for approximately 5 min. Verapamil, lidocaine and propranolol at 10 µM concentration were utilised as reference compounds in this experiment. Microsomes were also pre-warmed at 37°C before the addition of 30 µL to each well of the plate resulting in a final concentration of 1 mg/mL. The reaction was terminated at the appropriate time point (0 or 30 min) by addition of 60 µL of ice-cold 0.3 M trichloroacetic acid (TCA) per well. The plates

were centrifuged for 10 min at 112 x g and the supernatant fraction transferred to a fresh U-bottom 96-well plate. Plates were sealed and frozen at -20 °C prior to MS analysis. LC-MS/MS was used to quantify the peak area response of each compound before and after incubation with liver microsomes using MS tune settings established and validated for each compound. These peak intensity measurements were used to calculate the % remaining after incubation with microsomes for each hit compound.

6.6. Cellular 11β-HSD1 enzyme inhibition assay

The cellular 11β-HSD1 enzyme inhibition assay was performed using HEK293 cells stably transfected with the human 11β-HSD1 gene. Cells were incubated with substrate (cortisone) and product (cortisol) was determined by LC/MS. Cells were plated at 2 x 10^4 cells/well in a 96-well poly-D-lysine coated tissue culture microplate (Greiner Bio-one) and incubated overnight at 37 °C in 5% CO_2 95% O_2. Compounds to be tested were solubilized in 100% DMSO at 10 mM and serially diluted in water and 10% DMSO to final concentration of 10 µM in 10% DMSO. 10 µL of each test dilution and 10 µL of 10% DMSO (for low and high control) were dispensed into the well of a new 96-well microplate (Greiner Bio-one). Medium was removed from the cell assay plate and 100 µL of DMEM solution (containing 1% penicillin, 1% streptomycin and 300 nM cortisone) added to each well. Cells were incubated for 2 h at 37 °C in 5% CO_2 95% O_2. Following incubation, medium was removed from each well into an eppendorf containing 500 µL of ethyl acetate, mixed by vortex and incubated at rt for 5 min. A calibration curve of known concentrations of cortisol in assay medium was also set up and added to 500 µL of ethyl acetate, vortexed and incubated as above. The supernatant of each eppendorf was removed to a 96-deep-well plate and dried down under liquid nitrogen at 65 °C. Each well was solubilised in 100 µL 70:30 H_2O:ACN and removed to a 96-well V-bottomed plate for LC/MS analysis. Separation was carried out on a sunfire 150 x 2.1 mm, 3.5 µM column using a H_2O:ACN gradient profile. Typical retention times were 2.71 min for cortisol and 2.8 min for cortisone. The peak area was calculated and the concentration of each compound determined from the calibration curve.

6.7. Cellular 11β-HSD2 Enzyme Inhibition Assay

For measurement of inhibition of 11β-HSD2, HEK293 cells stably transfected with the full-length gene coding for human 11β-HSD2 were used. The protocol was the same as for the cellular 11β-HSD1 enzyme inhibition assay, only changing the substrate, this time cortisol, and the concentrations of the tested compounds, 10, 1 and 0.1 µM.

6.8. Parallel Artificial Membrane Permeation Assays- Blood-Brain Barrier (PAMPA-BBB)

To evaluate the brain penetration of the different compounds, a parallel artificial membrane permeation assay for blood-brain barrier was used, following the method described by Di [50]. The in vitro permeability (P_e) of fourteen commercial drugs through lipid extract of porcine brain membrane together with the test compounds were determined. Commercial drugs and assayed compounds were tested using a mixture of PBS:EtOH (70:30). Assay validation was made by comparing the experimental permeability with the reported values of the commercial drugs by bibliography and lineal correlation between experimental and reported permeability of the fourteen commercial drugs using the parallel artificial membrane permeation assay was evaluated ($y = 1.5366x -0.9672$; $R_2=0.9382$). From this equation and taking into account the limits established by Di et al. for BBB permeation [50], we established the ranges of permeability as compounds of high BBB permeation (CNS +): P_e (10^{-6} cm s^{-1}) > 5.179; compounds of low BBB permeation (CNS −): P_e (10^{-6} cm s^{-1}) < 2.106 and compounds of uncertain BBB permeation (CNS ±): $5.179 > P_e$ (10^{-6} cm s^{-1}) > 2.106.

6.9. Pharmacokinetic study

All the animal experiments were performed according to the protocols approved by the Animal Experimentation Ethical Committee of Universitat Autònoma de Barcelona and by the Animal Experimentation Commission of the Generalitat de Catalunya (Catalan Government). Male CD-1 mice (20-25 g) purchased from Envigo Laboratories were used. Compound **23** was dissolved in cyclodextrin 10% at 3 mg/mL to give a clear solution. After oral administration (21 mg/kg, 10 mL/Kg), blood (0.6 mL) was collected from cava vein using a syringe (23G needle) rinsed with 5% EDTA(K2) at 0, 0.5, 1, 3, 5 and 24 (3 animals/point). Each blood sample was immediately transferred to a tube containing 40 μL of water with 5% EDTA. Blood samples were centrifuged at 10000 g for 5 minutes and plasma samples were stored at −20 °C until analysis of compound concentration by UPLC-MS/MS. Brains were transcardially perfused with 10 mL of saline, removed, frozen in liquid N_2 and stored at −80 °C until analysis of the compound concentration by UPLC-MS/MS.

6.10. In vivo study

6.10.1. Animals.

SAMP8 mice 12 months old (n=12) were randomized in 2 experimental groups (control, n=4; treated, n=8), and additional group 2 months old (n=4) were planned as a young population. Mice were used with free access to food and water, under standard temperature conditions ($22 \pm 2°C$) and 12-h:12-h light-dark cycles (300 lx/0 lx). Compound **23** was administered dissolved in tap water and PEG400 (2% final concentration) yielding a dose of 21 mpk for 4 weeks. The dose was selected based on the IC_{50} value of **23** and our previous expertise in *in vivo* studies with other 11β-HSD1 inhibitors [20-21]. To maintain the correct dose along the treatment period, once a week the weight of the animals and the quantity of water that they drank were measured. Therefore, we adjusted the concentration (mg/mL) of the compound **23** in the drink bottle to achieve the correct dose of compound (mpk) to be administered to mice. Studies were performed in accordance with the institutional guidelines for the care and use of laboratory animals established by the Ethical Committee for Animal Experimentation at the University of Barcelona.

6.10.2. Novel Object Recognition Test (NORT).

The test was conducted in a 90-degree, two-arm, 25-cm-long, 20-cm-high maze. Light intensity in the middle of the field was 30 lux. The objects to be discriminated were plastic figures (object A, 5.25-cm-high, and object B, 4.75-cm-high). First, mice were individually habituated to the apparatus for 10 min per day during 3 days. On day 4, they were submitted to a 10-min acquisition trial (first trial), during which they were placed in the maze in the presence of two identical novel objects (A+A or B+B) placed at the end of each arm. A 10-min retention trial (second trial) occurred 2 h (short term memory) or 24 h (long term memory) later. During this second trial, objects A and B were placed in the maze, and the times that the animal took to explore the new object (tn) and the old object (to) were recorded. A Discrimination index (DI) was defined as (tn-to)/(tn+to). In order to avoid object preference biases, objects A and B were counterbalanced so that one half of the animals in each experimental group were first exposed to object A and then to object B, whereas the other one half first saw object B and then object A was presented. The maze, the surface, and the objects were cleaned with 96º ethanol between the animals' trials so as to eliminate olfactory cues.

6.10.3. Brain isolation and Western blot analysis.

Mice were euthanized 1 day after the last NORT trial was conducted, and brain quickly removed from the skull. Hippocampus were dissected and frozen in powdered dry ice

and maintained at −80 °C for further use. Tissue samples were homogenized in lysis buffer containing phosphatase and protease inhibitors (Cocktail II, Sigma), and cytosol and nuclear fractions were obtained as described elsewhere. Protein concentration was determined by the Bradford method. 20 μg of protein were separated by Sodium dodecyl sulfate-Polyacrylamide gel electrophoresis (SDS-PAGE) (8-15%) and transferred onto Polyvinylidene diflouride (PVDF) membranes (Millipore). The membranes were blocked in 5% non-fat milk in Tris-buffered saline containing 0.1% Tween 20 (TBS-T) for 1 h at rt, followed by overnight incubation at 4°C with primary antibodies against PSD95 (1:1,000, ab18258/Abcam), IDE (1:1,000, ab32216/Abcam) and APP C-Terminal Fragment (1:1,000, C1/6.1/Covance) diluted in TBS-T and 5% bovine serum albumin (BSA). GAPDH (1:2,000, Millipore) was used as a control protein charge. Membranes were then washed and incubated with secondary antibodies for 1 h at rt. Immunoreactive proteins were visualized utilizing an Enhanced chemiluminescence-based detection kit (ECL kit; Millipore) and digital images were acquired employing a ChemiDoc XRS+System (BioRad). Band intensities were quantified by densitometric analysis using Image Lab software (BioRad) and values were normalized to GAPDH.

6.10.4. RNA extraction and gene expression determination.

Total RNA isolation was carried out by means of Trizol reagent following the manufacturer's instructions. RNA content in the samples was measured at 260 nm, and sample purity was determined by the A260/280 ratio in a NanoDrop™ ND-1000 (Thermo Scientific). Samples were also tested in an Agilent 2100B Bioanalyzer (Agilent Technologies) to determine the RNA integrity number. Reverse transcription-Polymerase chain reaction (RT-PCR) was performed as follows: 2 μg of messenger RNA (mRNA) was reverse-transcribed using the High Capacity complementary DNA (cDNA) Reverse Transcription kit (Applied Biosystems). Real-time quantitative PCR (qPCR) was utilized to quantify the mRNA expression of inflammatory genes Interleukin 6 (*IL-6*) and inducible nitric oxide synthase (*iNOS*). Normalization of expression levels was performed with *Actin* for SYBER Green. The primers were as follows: for *IL-6*, forward 5'-ATCCAGTTGCCTTCTTGGGACTGA-3' and reverse 5'-TAAGCCTCCGACTTGTGAAGTGGT-3', for *iNOS*, forward 5'-GGCAGCCTGTGAGACCTTTG-3' and reverse 5'- GAAGCGTTTCGGGATCTGAA-

3', for *Actin*, forward 5'-CAACGAGCGGTTCCGAT-3' and reverse 5'-GCCACAGGTTCCATACCCA-3'.

Real-time PCR was performed on the Step One Plus Detection System (Applied Biosystems) employing the SYBR Green PCR Master Mix (Applied Biosystems). Each reaction mixture contained 7.5 μL of cDNA, whose concentration was 2 μg/μL, 0.75 μL of each primer (whose concentration was 100 nM), and 7.5 μL of SYBR Green PCR Master Mix (2X).

Data were analysed utilizing the comparative Cycle threshold (Ct) method (ΔΔCt), where the actin transcript level was utilized to normalize differences in sample loading and preparation. Each sample (n = 4-8) was analysed in triplicate, and the results represented the n-fold difference of transcript levels among different samples.

6.10.5. Data analysis.

Data are expressed as the mean ± Standard Error of the Mean (SEM). Data analysis was conducted using GraphPad Prism® ver. 6 statistical software. Means were compared with one-way Analysis of Variance (ANOVA) and Tukey post hoc analysis.

Acknowledgements

References

(1) Meaney, M. J.; O'Donnell, D.; Rowe, W.; Tannenbaum, B.; Steverman, A.; Walker, M.; Nair, N. P. V.; Lupien, S. Individual differences in hypothalamic- pituitary-

adrenal activity in later life and hippocampal aging. *Exp. Gerontol.* **1995**, *30*, 229-251.

(2) Yau, J. L.; Olsson, T.; Morris, R. G.; Meaney, M. J.; Seckl, J. R. Glucocorticoids, hippocampal corticosteroid receptor gene expression and antidepressant treatment: relationship with spatial learning in young and aged rats. *Neuroscience* **1995**, *66*, 571-581.

(3) Lupien, S. J.; de Leon, M.; de Santi, S.; Convit, A.; Tarshish, C.; Nair, N. P. V.; Thakur, M.; McEwen, B. S.; Hauger, R. L.; Meaney, M. J. Cortisol levels during human aging predict hippocampal atrophy and memory deficits. *Nat. Neurosci.* **1998**, *1*, 69-73.

(4) Reynolds, R. M. Glucocorticoid excess and the developmental origins of disease: two decades of testing the hypothesis. *Psychoneuroendocrinology* **2013**, *38*, 1-11.

(5) Peskind, E. R.; Wilkinson, C. W.; Petrie, E. C.; Schellenberg, G. D.; Raskind, M. A. Increased CSF cortisol in AD is a function of APOE genotype. *Neurology* **2001**, *56*, 1094-1098.

(6) Cernansky, J. G.; Dong, H.; Fagan, A. M.; Wang, L.; Xiong, C.; Holtzman, D. M.; Morris, J. C. Plasma cortisol and progression of dementia in subjects with Alzheimer-type dementia. *Am. J. Psychiatry* **2006**, *163*, 2164-2169.

(7) Green, K. N.; Billings, L. M.; Roozendaal, B.; McGaugh, J. L.; LaFerla, F. M. Glucocorticoids increase amyloid-β and tau pathology in a mouse model of Alzheimer's disease. *J. Neurosci.* **2006**, *26*, 9047-9056.

(8) Holmes, M. C.; Yau, J. L.; Kotelevtsev, Y.; Mullins, J. J.; Seckl, J. R.; 11 beta-hydroxysteroid dehydrogenases in the brain: two enzymes two roles. *Ann. N.Y. Acad. Sci.* **2003**, *1007*, 357-366.

(9) Holmes, M. C.; Seckl, J. R. The role of 11 beta-hydroxysteroid dehydrogenases in the brain. *Mol. Cell. Endocrinol*. **2006**, *248*, 9-14.

(10) Wyrwoll, C. S.; Holmes, M. C.; Seckl, J. R. 11β-Hydroxysteroid dehydrogenases and the brain: from zero to hero, a decade of progress. *Front. Neuroendocrinol.* **2011**, *32*, 265-286.

(11) Moisan, M.-P.; Seckl, J. R.; Edwards, C. R. W. 11β-hydroxysteroid dehydrogenase bioactivity and messenger RNA expression in rat forebrain: localization in hypothalamus, hippocampus and cortex. *Endocrinology* **1990**, *127*, 1450-1455.

(12) Pelletier, G.; Luu-The, V.; Li, S.; Bujold, G.; Labrie, F. Localization and glucocorticoid regulation of 11beta-hydroxysteroid dehydrogenase type 1 mRNA in the male mouse forebrain. *Neuroscience* **2007**, *145*, 110-115.

(13) Sandeep, T. C.; Yau, J. L.; MacLullich, A. M.; Noble, J.; Deary, I. J.; Walker, B. R.; Seckl, J. R. 11Beta-hydroxysteroid dehydrogenase inhibition improves cognitive function in healthy elderly men and type 2 diabetics. *Proc. Natl. Acad. Sci. U. S. A.* **2004**, *101*, 6734-6739.

(14) Brown, R. W.; Diaz, R.; Robson, A. C.; Kotelevtsev, Y. V.; Mullins, J. J.; Kaufman, M. H.; Seckl, J. R. The ontogeny of 11 beta-hydroxysteroid dehydrogenase type 2 and mineralocorticoid receptor gene expression reveal intricate control of glucocorticoid action in development. *Endocrinology* **1996**, *137*, 794-797.

(15) Brown, R. W.; Kotolevtsev, Y.; Leckie, C.; Lindsay, R. S.; Lyons, V.; Murad, P.; Mullins, J. J.; Chapman, K. E.; Edwards, C. R. W.; Seckl, J. R. Isolation and cloning of human placental 11β-hydroxysteroid dehydrogenase-2 cDNA. *Biochem. J*. **1996**, *313*, 1007-1017.

(16)   Wyrwoll, C.; Keith, M.; Noble, J.; Stevenson, P. L.; Bomball, V.; Crombie, S.; Evans, L. C.; Bailey, M. A.; Wood, E.; Seckl, J. R.; Holmes, M. C. Fetal brain 11β-hydroxysteroid dehydrogenase type 2 selectively determines programming of adult depressive-like behaviors and cognitive function, but not anxiety behaviors in male mice. *Psychoneuroendocrinology* **2015**, *59*, 59-70.

(17)   Holmes, M .C.; Carter, R. N.; Noble, J.; Chitnis, S.; Dutia, A.; Paterson, J. M.; Mullins, J. J.; Seckl, J. R.; Yau, J. L. 11β-hydroxysteroid dehydrogenase type 1 expression is increased in the aged mouse hippocampus and parietal cortex and causes memory impairments. *J. Neurosci*. **2010**, *30*, 6916-6920.

(18)   Yau, J. L.; Noble, J.; Kenyon, C. J.; Hibberd, C.; Kotelevtsev, Y.; Mullins, J. J.; Seckl, J. R. Lack of tissue glucocorticoid reactivation in 11beta-hydroxysteroid dehydrogenase type 1 knockout mice ameliorates age-related learning impairments. *Proc. Natl. Acad. Sci U. S. A.* **2001**, *98*, 4716-4721.

(19)   Sooy, K; Webster, S. P.; Noble, J.; Binnie, M.; Walker, B. R.; Seckl, J. R.; Yau, J. L. W. Partial deficiency or short-term inhibition of 11β-hydroxysteroid dehydrogenase type 1 improves cognitive function in aging mice. *J. Neurosci*. **2010**, *30*, 13867-13872.

(20)   Wheelan, N.; Webster, S. P.; Kenyon, C. J.; Caughey, S.; Walker, B. R.; Holmes, M. C.; Seckl, J. R.; Yau, J. L. W. Short-term inhibition of 11β-hydroxysteroid dehydrogenase type 1 reversibly improves spatial memory but persistently impairs contextual fear memory in aged mice. *Neuropharmacol*. **2015**, *91*, 71-76.

(21)   Sooy, K.; Noble, J.; McBride, A.; Binnie, M.; Yau, J. L. W.; Seck, J. R.; Walker, B. R.; Webster, S. P. Cognitive and disease-modifying effects of 11β-

hydroxysteroid dehydrogenase type 1 inhibition in male Tg2576 mice, a model of Alzheimer's Disease. *Endocrinology* **2015**, *156*, 4592-4603.

(22)   Mohler, E. G.; Browman, K. E.; Roderwald, V. A.; Cronin, E. A.; Markosyan, S.; Bitner, R. S.; Strakhova, M. I.; Drescher, K. U.; Hornberger, W.; Rohde, J. J.; Brune, M. E.; Jacobson, P. B.; Rueter, L. E. Acute inhibition of 11β-hydroxysteroid dehydrogenase type-1 improves memory in rodent models of cognition. *J. Neurosci.* **2011**, *31*, 5406-5413.

(23)   Yau, J. L. W.; Seckl, J. R. Local amplification of glucocorticoids in the aging brain and impaired spatial memory. *Front. Aging Neurosci.* **2012**, *4*, 24.

(24)   Morley, J. E.; Farr, S. A.; Kumar, V. B.; Armbrecht, H. J. The SAMP8 mouse: a model to develop therapeutic interventions for Alzheimer's disease. *Curr. Pharm. Des.* **2012**, *18*, 1123-1130.

(25)   Morley, J. E.; Armbrecht, H. J.; Farr, S. A.; Kumar, V. B. The senescence accelerated mouse (SAMP8) as a model for oxidative stress and Alzheimer's disease. *Biochim. Biophys. Acta* **2012**, *1822*, 650-656.

(26)   Olson, S.; Aster, S. D.; Brown, K.; Carbin, L.; Graham, D. W.; Hermanowski-Vosatka, A.; LeGrand, C. B.; Mundt, S. S.; Robbins, M. A.; Schaeffer, J. M.; Slossberg, L. H.; Szymonifka, M. J.; Thieringer, R.; Wright, S. D.; Balkovec, J. M. Adamantyl triazoles as selective inhibitors of 11beta-hydroxysteroid dehydrogenase type 1. *Bioorg. Med. Chem. Lett.* **2005**, *15*, 4359-4362.

(27)   Sorensen, B.; Rohde, J.; Wang, J.; Fung, S.; Monzon, K.; Chiou, W.; Pan, L.; Deng, X.; Stolarik, D.; Frevert, E. U.; Jacobson, P.; Link, J. T. Adamantane 11-beta-HSD-1 inhibitors: Application of an isocyanide multicomponent reaction. *Bioorg. Med. Chem. Lett.* **2006**, *16*, 5958-5962.

(28)   Becker, C. L.; Engstrom, K. M.; Kerdesky, F. A.; Tolle, J. C.; Wagaw, S. H.; Wang, W. A convergent process for the preparation of adamantane 11b-HSD1 inhibitors. *Org. Process Res. Dev.* **2008**, *12*, 1114-1118.

(29)   Scott, J. S.; Barton, P.; Bennett, S. N. L.; deSchoolmeester, J.; Godfrey, L.; Kilgour, E.; Mayers, R. M.; Packer, M. J.; Rees, A.; Schofield, P.; Selmi, N.; Swales, J. G.; Whittamore, P. R. O. Reduction of acyl glucuronidation in a series of acidic 11beta-hydroxysteroid dehydrogenase type 1 (11beta-HSD1) inhibitors: the discovery of AZD6925. *Med. Chem. Commun.* **2012**, *3*, 1264-1269.

(30)   Scott, J. S.; deSchoolmeester, J.; Kilgour, E.; Mayers, R. M.; Packer, M. J.; Hargreaves, D.; Gerhardt, S.; Ogg, D. J.; Rees, A.; Selmi, N.; Stocker, A.; Swales, J. G.; Whittamore, P. R. O. Novel acidic 11β-hydroxysteroid dehydrogenase type 1 (11β-HSD1) inhibitor with reduced acyl glucuronide liability: the discovery of 4-[4-(2-adamantylcarbamoyl)-5-tert-butyl-pyrazol-1-yl]benzoic acid (AZD8329). *J. Med. Chem.* **2012**, *55*, 10136-10147.

(31)   Venier, O.; Pascal, C.; Braun, A.; Namane, C.; Mougenot, P.; Crespin, O.; Pacquet, F.; Mougenot, C.; Monseau, C.; Onofri, B.; Dadji-Faïhun, R.; Leger, C.; Ben-Hassine, M.; Van-Pham, T.; Ragot, J.-L.; Philippo, C.; Farjot, G.; Noah, L.; Maniani, K.; Boutarfa, A.; Nicolaï, E.; Guillot, E.; Pruniaux, M.-P.; Güssregen, S.; Engel, C.; Coutant, A.-L.; de Miguel, B.; Castro, A. Discovery of SAR184841, a potent and long-lasting inhibitor of 11β-hydroxysteroid dehydrogenase type 1, active in a physiopathological animal model of T2D. *Bioorg. Med. Chem. Lett.* **2013**, *23*, 2414-2421.

(32)   Park, S. B.; Jung, W. H.; Kang, N. S.; Park, J. S.; Bae, G. H.; Kim, H. Y.; Rhee, S. D.; Kang, S. K.; Ahn, J. H.; Jeong, H. G.; Kim, K. Y. Anti-diabetic and anti-

inflammatory effect of a novel selective 11β-HSD1 inhibitor in the diet-induced obese mice. *Eur. J. Pharmacol.* **2013**, *721*, 70-79.

(33)   Okazaki, S.; Takahashi, T.; Iwamura, T.; Nakaki, J.; Sekiya, Y.; Yagi, M.; Kumagai, H.; Sato, M.; Sakami, S.; Nitta, A.; Kawai, K.; Kainoh, M. HIS-388, a Novel Orally Active and Long-Acting 11β-Hydroxysteroid Dehydrogenase Type 1 Inhibitor, Ameliorates Insulin Sensitivity and Glucose Intolerance in Diet-Induced Obesity and Nongenetic Type 2 Diabetic Murine Models. *J. Pharmacol. Exp. Ther.* **2014**, *351*, 181-189.

(34)   Byun, S. Y.; Shin, Y. J.; Nam, K. Y.; Hong, S. P.; Ahn, S. K. A novel highly potent and selective 11β-hydroxysteroid dehydrogenase type 1 inhibitor, UI-1499. *Life Sci.* **2015**, *120*, 1-7.

(35)   Gibbs, J. P.; Emery, M. G.; McCaffery, I.; Smith, B.; Gibbs, M. A.; Akrami, A.; Rossi, J.; Paweletz, K.; Gastonguay, M. R.; Bautista, E.; Wang, M.; Perfetti, R.; Daniels, O. Population Pharmacokinetic/Pharmacodynamic Model of Subcutaneous Adipose 11β-Hydroxysteroid Dehydrogenase Type 1 (11β-HSD1) Activity After Oral Administration of AMG 221, a Selective 11β-HSD1 Inhibitor. *J. Clin. Pharmacol.* **2011**, *51*, 830–841.

(36)   Shah, S.; Hermanowski-Vosatka, A.; Gibson, K.; Ruck, R. A.; Jia, G.; Zhang, J.; Hwang, P. M. T.; Ryan, N. W.; Langdon, R. B.; Feig, P. U. Efficacy and safety of the selective 11β-HSD1 inhibitors MK-0736 and MK-0916 in overweight and obese patients with hypertension. *J. Am. Soc. Hypertens.* **2011**, *5*, 166-176.

(37)   Duque, M. D.; Camps, P.; Profire, L.; Montaner, S.; Vázquez, S.; Sureda, F. X.; Mallol, J.; López-Querol, M.; Naesens, L.; De Clercq, E.; Prathalingam, S. R.;

Kelly, J. M. Synthesis and pharmacological evaluation of (2-oxaadamantan-1-yl)amines. *Bioorg. Med. Chem.* **2009**, *17*, 3198-3206.

(38)   Duque, M. D.; Ma, C.; Torres, E.; Wang, J.; Naesens, L.; Juárez-Jiménez, J.; Camps, P.; Luque, F. J.; DeGrado, W. F.; Lamb, R. A.; Pinto, L. H.; Vázquez, S. Exploring the size limit of templates for inhibitors of the M2 ion channel of influenza A virus. *J. Med. Chem.* **2011**, *54*, 2646-2657.

(39)   Rey-Carrizo, M.; Torres, E.; Ma, C.; Barniol-Xicota, M.; Wang, J.; Wu, Y.; Naesens, L.; Degrado, W. F.; Lamb, R. A.; Pinto, L. H.; Vázquez, S. 3-Azatetracyclo[5.2.1.1^{5,8}.0^{1,5}]undecane derivatives: from wild-type inhibitors of the M2 ion channel of influenza A virus to derivatives with potent activity against the V27A mutant. *J. Med. Chem.* **2013**, *56*, 9265-9274.

(40)   Rey-Carrizo, M.; Barniol-Xicota, M.; Ma, C.; Frigolé-Vivas, M.; Torres, E.; Naesens, L.; Llabrés, S.; Juárez-Jiménez, J.; Luque, F. J.; Degrado, W. F.; Lamb, R. A.; Pinto, L. H.; Vázquez, S. Easily accessible polycyclic amines that inhibit the wild-type and amantadine-resistant mutants of the M2 channel of the influenza A virus. *J. Med. Chem.* **2014**, *57*, 5738-5747.

(41)   Torres, E.; Leiva, R.; Gazzarrini, S.; Rey-Carrizo, M.; Frigolé-Vivas, M.; Moroni, A.; Naesens, L.; Vázquez, S. Azapropellanes with Anti-Influenza A Virus activity. *ACS Med. Chem. Lett.* **2014**, *5*, 831-836.

(42)   Leiva, R.; Gazzarrini, S.; Esplugas, R.; Moroni, A.; Naesens, L.; Sureda, F. X.; Vázquez, S. Ritter reaction-mediated syntheses of 2-oxaadamantan-5-amine, a novel amantadine analog. *Tetrahedron Lett*. **2015**, *56*, 1272-1275.

(43)   Duque, M. D.; Camps, P.; Torres, E.; Valverde, E.; Sureda, F. X.; López-Querol, M.; Camins, A.; Prathalingam, S. R.; Kelly, J. M.; Vázquez, S. New oxapolycyclic

cage amines with NMDA receptor antagonist and trypanocidal activities. *Bioorg. Med. Chem.* **2010**, *18*, 46-57.

(44)   Torres, E.; Duque, M. D.; López-Querol, M.; Taylor, M. C.; Naesens, L.; Ma, C.; Pinto, L. H.; Sureda, F. X.; Kelly, J. M.; Vázquez, S. Synthesis of benzopolycyclic cage amines: NMDA receptor antagonist, trypanocidal and antiviral activities. *Bioorg. Med. Chem.* **2012**, *20*, 942-948.

(45)   Valverde, E.; Sureda, F. X.; Vázquez, S. Novel benzopolyclic amines with NMDA receptor antagonist activity. *Bioorg. Med. Chem.* **2014**, *22*, 2678-2683.

(46)   Valverde, E.; Seira, C.; McBride, A.; Binnie, M.; Luque, F. J.; Webster, S. P.; Bidon-Chanal, A.; Vázquez, S. Searching for novel applications of the benzohomoadamantane scaffold in medicinal chemistry: Synthesis of novel 11β-HSD1 inhibitors. *Bioorg. Med. Chem.* **2015**, *23*, 7607-7617.

(47)   Cheng, H.; Hoffman, J.; Le, P.; Nair, S. K.; Cripps, S.; Matthews, J.; Smith, C.; Yang, M.; Kupchinsky, S.; Dress, K.; Edwards, M.; Cole, B.; Walters, E.; Loh, C.; Ermolieff, J.; Fanjul, A.; Bhat, G. B.; Herrera, J.; Pauly, T.; Hosea, N.; Paderes, G.; Rejto, P. The development and SAR of pyrrolidine carboxamide 11β-HSD1 inhibitors. *Bioorg. Med. Chem. Lett.* **2010**, *20*, 2897-2902.

(48)   Leiva, R.; Seira, C.; McBride, A.; Binnie, M.; Bidon-Chanal, A.; Luque, F. J.; Webster, S. P.; Vázquez, S. Novel 11β-HSD1 inhibitors: effects of the C-1 vs C2-substitution and of the introduction of an oxygen atom in the adamantane scaffold. *Bioorg. Med. Chem. Lett.* **2015**, *25*, 4250-4253.

(49)   During the writing of this manuscript it has been reported the discovery and the results of Phase 1 clinical trials of UE2343, a brain-penetrant 11β-HSD1 inhibitor featuring a pyrrolidine unit embedded in a tropane core. The compound is being developed by Actinogen Medical for the treatment of Alzheimer's disease. See,

Webster, S. P.; McBride, A.; Binnie, M.; Sooy, K.; Seckl, J. R.; Andrew, R.; Pallin, T. D.; Hunt, H. J.; Perrior, T. R.; Ruffles, V. S.; Ketelbey, J. W.; Boyd, A.; Walker, B. R. Selection and early clinical evaluation of the brain-penetrant 11β-hydroxysteroid dehydrogenase type 1 (11β-HSD1) inhibitor UE2343 (Xanamem™). *British J. Pharmacol.* **2017**, *174*, 396-408.

(50)   Di, L.; Kerns, E. H.; Fan, K.; McConnell, O. J.; Carter, G. T. High throughput artificial membrane permeability assay for blood-brain barrier. *Eur. J. Med. Chem.* **2003**, *38*, 223-232.

(51)   Takeda, T. Senescence-accelerated mouse (SAM) with special references to neurodegeneration models, SAMP8 and SAMP10 mice. *Neurochem. Res.* **2009**, *34*, 639-659.

(52)   Pallàs, M. Senescence-accelerated mice P8: a tool to study brain aging and Alzheimer's disease in a Mouse Model. *ISRN Cell Biology* 2012, 917167.

(53)   Griñan-Ferré, C.; Palomera-Ávalos, V.; Puigoriol-Illamola, D.; Camins, A.; Porquet, D.; Plá, V.; Aguado, F.; Pallàs, M. Behaviour and cognitive changes correlated with hippocampal neuroinflammaging and neuronal markers in female SAMP8, a model of accelerated senescence. *Exp. Gerontol.* **2016**, *80*, 57-69.

(54)   Antunes, M.; Biala, G. The novel object recognition memory: neurobiology, test procedure, and its modifications. *Cogn. Process.* **2012**, *13*, 93-110.

(55)   Murphy, M. P.; LeVine III, H. Alzheimer's disease and the amyloid-beta peptide. *J. Alzheimers Dis.* **2010**, *19*, 311-323.

(56)   Kim, M.; Hersh, L. B.; Leissring, M. A.; Ingelsson, M.; Matsui, T.; Farris, W.; Lu, A.; Hyman, B. T.; Selkoe, D. J.; Bertram, L.; Tanzi, R. E. Decreased catalytic activity of the insulin-degrading enzyme in chromosome 10-linked Alzheimer Disease families. *J. Biol. Chem.* **2007**, *282*, 7825-7832.

(57)   Morley, J. E.; Farr, S. A.; Flood, J. F. Antibody to amyloid beta protein alleviates impaired acquisition, retention, and memory processing in SAMP8 mice. *Neurobiol. Learn. Mem.* **2002**, *78*, 125-138.

(58)   Culberson, C. F.; Wilder Jr., P. The synthesis of 2-aza-1,2-dihydrodicyclopentadienes. *J. Org. Chem.* **1960**, *25*, 1358-1362.

(59)   Fumimoto, M.; Okabe, K. Nouvelle méthode de synthése des dérivés d'ethano-4,7 polyhydroisoindoline. *Chem. Pharm. Bull.* **1962**, *10*, 714-718.

(60)   Friesner, R. A.; Murphy, R. B.; Repasky, M. P.; Frye, L. L.; Greenwood, J. R.; Halgren, T. A.; Sanschagrin, P. C.; Mainz, D. T. Extra precision Glide: Docking and scoring incorporating a model of hydrophobic enclosure for protein-ligand complexes. *J. Med. Chem.* **2006**, *49*, 6177-6196.

(61)   Goldberg, F. W.; Leach, A. G.; Scott, J. S.; Snelson, W. L.; Groombridge, S. D.; Donald, C. S.; Bennett, S. N. L.; Bodin, C.; Gutierrez, P. M.; Gyte, A. C. Free-Wilson and structural approaches to co-optimising human and rodent isoform potency for 11β-hydroxysteroid dehydrogenase type 1 (11β-HSD1) inhibitors. *J. Med. Chem.* **2012**, *55*, 10652-10661.

(62)   Jorgensen, W. L.; Chandrasekhar, J.; Madura, J. D.; Impey, R. W.; Klein, M. L. Comparison of simple potential functions for simulating liquid water. *J. Chem. Phys.* **1983**, *79*, 926-935.

(63)   Hornak, V.; Abel, R.; Okur, A.; Strockbine, B.; Roitberg, A.; Simmerling, C. Comparison of multiple Amber force fields and development of improved protein backbone parameters. *Proteins* **2006**, *65*, 712-725.

(64)   Lindorff-Larsen, K.; Piana, S.; Palmo, K.; Maragakis, P.; Klepeis, J. L.; Dror, R. O.; Shaw, D. E. Improved side-chain torsion potentials for the Amber ff99SB force field. *Proteins* **2010**, *78*, 1950-1958.

(65)   Wang, J.; Wolf, R. M.; Caldwell, J. W.; Kollman, P. A.; Case, D. A. Development and testing of a general force field. *J. Comp. Chem.* **2004**, *25*, 1157-1174.

(66)   Yau, J. L. W.; Wheelan, N.; Noble, J.; Walker, B. R.; Webster, S. P.; Kenyon, C. J.; Ludwig, M.; Seckl, J. R. Intrahippocampal glucocorticoids generated by 11β-HSD1 affect memory in aged mice. *Neurobiol. Aging* **2015**, *36*, 334-343

Appendix A. Supplementary data

Supplementary data related to this article can be found at http://